Preparation and characterization of magnetic nanoparticles

Author: Sheila Moratal Ruiz

Tutor: Santiago Ferrándiz Bou

UNIVERSIDAD POLITÉCNICA DE VALENCIA

UNIVERSITAT
POLITÈCNICA
DE VALÈNCIA
CAMPUS D'ALCOI

Content

Objectives

The aim of this report was the synthesis of magnetic nanoparticles and its potential applications through the co-precipitation method, more concretely through Massart synthesis. For this purpose, it was necessary to use different solutions in order to contrast the results. On the other hand, it would be necessary to apply a coating to prevent the degradation and agglomeration of the magnetic nanoparticles and also a stabilizing agent to avoid the agglomeration or clustering of the nanoparticles. Using the different dissolutions different size of nanoparticles will be obtained. Finally, the size of the particles will be compared for the choice of the best conditions that allow obtaining dispersed and stabilized magnetic nanoparticles.

1   Introduction

Magnetic nanoparticles are a class of nanoparticle that can be manipulated using magnetic fields. Such particles commonly consist of two components, a magnetic material, often iron, nickel and cobalt, and a chemical component that has functionality. While nanoparticles are smaller than 1 micrometer in diameter (typically 5–500 nanometers), the larger microbeads are 0.5–500 micrometer in diameter. Magnetic nanoparticle clusters that are composed of a number of individual magnetic nanoparticles are known as magnetic nanobeads with a diameter of 50–200 nanometers. Magnetic nanoparticle clusters are a basis for their further magnetic assembly into magnetic nanochains. The magnetic nanoparticles have been the focus of much research recently because they possess attractive properties which could see potential use in catalysis including nanomaterial-based catalysts, biomedicine and tissue specific targeting, magnetically tunable colloidal photonic crystals, microfluidics, magnetic resonance imaging, magnetic particle imaging, data storage, environmental remediation, nanofluids, and optical filters, defect sensor and cation sensors.

Magnetic nanoparticles are of great interest for researchers from a wide range of disciplines, including magnetic fluids, catalysis, biotechnology/biomedicine. While a number of suitable methods have been developed for the synthesis of magnetic nanoparticles of various different compositions, successful application of such magnetic nanoparticles in the areas listed above is highly dependent on the stability of the particles under a range of different conditions. In most of the envisaged applications, the particles perform

best when the size of the nanoparticles is below a critical value, which is dependent on the material but is typically around 10–20 nm. Then each nanoparticle becomes a single magnetic domain and shows superparamagnetic behavior when the temperature is above the so-called blocking temperature. Such individual nanoparticles have a large constant magnetic moment and behave like a giant paramagnetic atom with a fast response to applied magnetic fields with negligible remanence (residual magnetism) and coercivity (the field required to bring the magnetization to zero). These features make superparamagnetic nanoparticles very attractive for a broad range of biomedical applications because the risk of forming agglomerates is negligible at room temperature.

However, an unavoidable problem associated with particles in this size range is their intrinsic instability over longer periods of time. Such small particles tend to form agglomerates to reduce the energy associated with the high surface area to volume ratio of the nanosized particles. Moreover, naked metallic nanoparticles are chemically highly active, and are easily oxidized in air, resulting generally in loss of magnetism and dispersibility. For many applications it is thus crucial to develop protection strategies to chemically stabilize the naked magnetic nanoparticles against degradation during or after the synthesis. These strategies comprise grafting of or coating with organic species, including surfactants or polymers, or coating with an inorganic layer, such as silica or carbon. It is noteworthy that in many cases the protecting shells not only stabilize the nanoparticles, but can also be used for further functionalization, for instance with other nanoparticles or various ligands, depending on the desired application.

Functionalized nanoparticles are very promising for applications in catalysis, biolabeling, and bioseparation. Especially in liquid-phase catalytic reactions, such small and magnetically separable particles may be useful as quasihomogeneous systems that combine the advantages of high dispersion, high reactivity, and easy separation [1].

2 Materials and properties

A continuation the properties of the materials used during the synthesis will be described.

2.1 Iron(III) Chloride Hexahydrate (FeCl₃·6H₂O)

Table 1: Properties of FeCl₃·6H₂O

Physical and chemical properties	
Physical state	Solid.
Appearance	Crystalline solid. Grains.
Molecular mass	270.32 g/mol
Colour	Brown-yellow.
pH	2
Melting point	37 °C
Boiling point	280 °C
Relative density	1.66
Solubility	Soluble in water. Soluble in ethanol. Soluble in ether. Soluble in acetone. Soluble in methanol. Water: 92 g/100ml (20 °C).
Reactivity	Reacts slowly with water/(moist) air: release of toxic and corrosive gases/vapours (hydrogen chloride). Reacts on exposure to water (moisture) with (some) metals: release of highly flammable gases/vapours (hydrogen). Decomposes on exposure to temperature rise: release of toxic and corrosive gases/vapours (chlorine, hydrogen chloride). Reacts violently with (some) bases: release of heat.
Other properties	Hygroscopic.

Figure 1:FeCl₃·6H₂O

2.2 Iron(II) Chloride Tetrahydrate (FeCl₂·4H₂O)

Table 2: Properties of FeCl₂·4H₂O

Physical and chemical properties	
Physical state	Solid.
Appearance	Powder. Grains.
Molecular mass	198.81 g/mol
Colour	Yellow to green
pH	2.5
Melting point	105 °C
Boiling point	1026 °C
Relative density	1.96
Solubility	Water: 160 g/100ml (20 °C).
Stability	Air, moisture and light-sensitive. Incompatible with strong oxidizing agents, most common metals.

Figure 2: FeCl₂·4H₂O

2.3 Gum Arabic

A water-soluble gum commonly used in binding media of paints. Gum arabic is the amorphous exudate from the stem of several species of Acacia trees, especially Acacia senegal and Acacia arabica, found in tropical and subtropical areas of the world. Most gum arabic comes from the sub-Sahara region in Africa. Gum arabic contains arabinose, galactose, rhamnose, and glucuronic acid. It is sold in the form of round lumps, granules, thin flakes or as a powder; all of which may be white or slightly yellowish. Gum arabic is completely soluble in hot and cold water, yielding a viscous solution. However, heating a gum arabic solution to the boiling point will cause it to darken and will change its adhesion properties. Aqueous solutions of gum arabic will precipitate or gel with the addition of ferric salts, borax, alcohol, or sodium silicate. Gum arabic is used in watercolor paints, inks, lithographs, and for textile sizing. The earliest known inks consisted of gum arabic and lampblack [3].

Figure 3: Gum Arabic

2.4 Essential oils

Essential oils are used extensively in aromatherapy and various traditional medicines. Due to the numerous health benefits of essential oils, they are increasingly being explored by the scientific community for the treatment of a variety of diseases including cancer, HIV, asthma, bronchitis, heart strokes, etc. There are more than 90 essential oils, and each has its own health benefits [4].

Figure 4: Flower of lavender.

Below is a list of properties of essential oils that are currently being widely used or researched:

- Anti-bacterial properties (lavender essential oil, lemon essential oil, lemongrass essential oil, patchouli essential oil, pine essential oil, spearmint essential oil, tea tree essential oil)

- Anti-fungal properties (cedarwood essential oil, myrrh essential oil, patchouli essential oil, peppermint essential oil, pine essential oil, spearmint essential oil, tea tree essential oil, thyme essential oil)

- Anti-irritant properties (lemon essential oil, ylang ylang essential oil)

- Anti-inflammatory properties (chamomile essential oil, frankincense essential oil, geranium essential oil, jasmine essential oil, myrrh essential oil, peppermint essential oil, sandalwood essential oil)

- Anti-microbal properties (peppermint essential oil, spearmint essential oil)

- Antioxidant properties (chamomile essential oil, rose otto essential oil)

- Anti-septic properties (carrot seed oil, cedarwood essential oil, chamomile essential oil, geranium essential oil, jasmine essential oil, lavender essential oil, myrrh essential oil, niaouli essential oil, orange essential oil, patchouli essential oil, peppermint essential oil, pine essential oil, tangerine essential oil, tea tree essential oil, thyme essential oil)

- Anti-viral properties (tea tree essential oil)

- Astringent properties (bergamont essential oil, cedarwood essential oil, chamomile essential oil, frankincense essential oil, geranium essential oil, lemon essential oil, myrrh essential oil, myrtle essential oil, neroli essential oil, sandalwood essential oil) [16].

2.4.1 Lavender essential oil

Lavender oil is extracted mostly from the flowers of the lavender plant, primarily through steam distillation. The flowers of lavender are fragrant in nature and have been used for making potpourri for centuries. Traditionally, lavender essential oil has also been used in making perfumes. The oil is very useful in aromatherapy and many aromatic preparations and combinations.

Today, lavender essential oil is frequently used in various forms including as an aromatherapy oil, in gels, infusions, lotions, and soaps. Some of the health benefits of lavender essential oil are exposed a continuation.

Bug Repellent

The smell of lavender essential oil is potent for many types of bugs like mosquitoes, midges, and moths. Apply some lavender oil on the exposed skin when outside to prevent these irritating bites. Furthermore, if you do happen to be bitten by one of those bugs, lavender essential oil has anti-inflammatory qualities that will reduce the irritation and the pain associated with bug bites.

Induces Sleep

Lavender essential oil induces sleep and is thus used as an alternative treatment for insomnia. Frequent studies on elderly patients have shown an increase in their sleep regularity when their normal sleep medication is replaced with some lavender essential oil being placed on their pillows. It has a relaxing impact on people; thereby, it often replaces modern medicines for sleep issues.

Relieves Stress and Anxiety

Lavender essential oil has a calming scent which makes it an excellent tonic for the nerves and anxiety issues. Therefore, it can also be helpful in treating migraines, headaches, depression, nervous tension and emotional stress. The refreshing aroma removes nervous exhaustion and restlessness while also increasing mental activity. It has a well-researched impact on the autonomic nervous system, which is why it is frequently used as a treatment for insomnia and also as a way to regulate heart-rate variability. One study showed that people taking tests showed a significant decrease in mental stress and anxiety, as well

as increased cognitive function when they inhaled lavender oil and rosemary oil before taking the test.

Treats Acne

Figure 5: Lavender essential oil.

According to dermatologists and aromatherapists, lavender essential oil is one of the most beneficial oils in the treatment of acne, which is a very uncomfortable and embarrassing condition that primarily affects young people as they move through puberty, but can also afflict adults. It is characterized by red, raised sores on the face and body that develop due to a bacterial infection near the sebum gland. When sebum cannot be properly secreted from the sebum glands on the face, it begins to build up, particularly because puberty stimulates extra sebum and bacteria feed off of it, creating a vicious cycle of irritation, infection, and visible sores that can result in serious scarring.

Lavender essential oil inhibits the bacteria that cause the initial infection, helps to regulate some of the over-excretion of sebum by hormonal manipulation and can reduce the signs of scarring after the acne has begun to heal. Adding a small amount of lavender essential oil to other skin creams or ointments can greatly increase the potential for relief and healing.

Relieves Pain

Lavender essential oil is known as an excellent remedy for various types of pains including those caused by sore and tense muscles, muscular aches,

rheumatism, sprains, backache, and lumbago. A regular massage with lavender oil can provide relief from pain in the joints. A study done on postoperative pain relief showed that combining lavender essential oil vapor into the oxygen significantly reduced the amount of pain experienced, versus those patients who were only revived with oxygen after a major surgery.

Stimulates Urine Flow

Lavender essential oil is good for urinary disorders because of its stimulating effect on urine production. Furthermore, it helps in restoring hormonal balance and reducing cystitis or inflammation of the urinary bladder. It also reduces associated cramps with these and other disorders.

Treats Respiratory Disorders

Lavender oil is widely used for various respiratory problems including throat infection, flu, cough, cold, asthma, sinus congestion, bronchitis, whooping cough, laryngitis, and tonsillitis. The oil is either used in the form of vapor or is applied to the skin of neck, chest, and back. It is also added to many vaporizers and inhalers that are commonly used for cold and cough. The stimulating nature of lavender essential oil can also loosen up the phlegm and relieve congestion associated with respiratory conditions, thus speeding up the recovery process and helping the body naturally eliminate phlegm and other unwanted material. The vapor of lavender essential oil also has antibacterial qualities which can battle respiratory tract infections.

Hair Care

Lavender essential oil is useful for hair care because it has been shown to be very effective on lice, lice eggs, and nits. Furthermore, lavender essential oil has also been shown to be very helpful in the treatment of hair loss, particularly for patients who suffer from alopecia, an autoimmune disease where the body rejects its own hair follicles. A Scottish study reported that more than 40% of alopecia patients in the study reported an increase in hair growth when they regularly rubbed lavender essential oil into their scalp. Therefore, lavender oil is sometimes recommended as a preventative measure for male pattern baldness.

Prevents Cancer

There is a significant research on the effects of lavender, in combination with other essential oils, as a way to prevent the occurrence of breast cancer in mice.

This could be an indication of an increased chance of lavender battling carcinogenic effects and the presence of cancer.

Improves Blood Circulation

Lavender essential oil is also good for improving circulation of blood in the body. Research suggests that aromatherapy using lavender oil has beneficial effects on coronary circulation. It also lowers blood pressure and is often used as a treatment for hypertension. This means that not only do the organs increase their levels of oxygenation, promoting muscle strength and health, but brain activity can have a noticeable boost, skin remains bright and flushed with blood, and the body is protected from the risks of heart attack and atherosclerosis often associated with poor blood circulation.

Aids in Digestion

Lavender oil is useful for digestion because it increases the mobility of food within the intestine. The oil also stimulates the production of gastric juices and bile, thus aiding in the treatment of indigestion, stomach pain, colic, flatulence, vomiting, and diarrhea.

Boosts Immunity

Regular use of lavender essential oil provides resistance to a variety of diseases. Lavender has antibacterial and antiviral qualities that make it perfect for defending the body against rare diseases like TB, typhoid, and diphtheria, according to early research in the 20th century.

Treats Eczema

It is used to treat various skin disorders such as acne, wrinkles, psoriasis, and other inflammatory conditions. It is commonly used to speed up the healing process of wounds, cuts, burns, and sunburns because it improves the formation of scar tissues. Lavender oil is also added to chamomile to treat eczema [17].

3 Synthesis of Magnetic Nanoparticles

Magnetic nanoparticles have been synthesized with a number of different compositions and phases, including iron oxides, such as Fe_3O_4 and γ-Fe_2O_3, pure metals, such as Fe and Co, spinel-type ferromagnets, such as $MgFe_2O_4$, $MnFe_2O_4$, and $CoFe_2O_4$, as well as alloys, such as $CoPt_3$ and FePt. In the last decades, much research has been devoted to the synthesis of magnetic nanoparticles. Especially during the last few years, many publications have described efficient synthetic routes to shape-controlled, highly stable, and monodisperse magnetic nanoparticles. Several popular methods including co-precipitation, thermal decomposition and/or reduction, micelle synthesis, hydrothermal synthesis, and laser pyrolysis techniques can all be directed at the synthesis of high-quality magnetic nanoparticles.

Table 3: Comparation between the synthesis methods

Synthetic method	Synthesis	Reaction temp. [°C]	Reaction period	Solvent	Surface-capping agents	Size distribution	Shape control	Yield
co-precipitation	very simple, ambient conditions	20–90	minutes	water	needed, added during or after reaction	relatively narrow	not good	high/ scalable
thermal decomposition	complicated, inert atmosphere	100–320	hours–days	organic compound	needed, added during reaction	very narrow	very good	high/ scalable
microemulsion	complicated, ambient conditions	20–50	hours	organic compound	needed, added during reaction	relatively narrow	good	low
hydrothermal synthesis	simple, high pressure	220	hours ca. days	water-ethanol	needed, added during reaction	very narrow	very good	medium

3.1 Co-Precipitation

Co-precipitation is a facile and convenient way to synthesize iron oxides (either Fe_3O_4 or γ-Fe_2O_3) from aqueous Fe^{2+}/Fe^{3+} salt solutions by the addition of a base under inert atmosphere at room temperature or at elevated temperature. The size, shape, and composition of the magnetic nanoparticles very much depends on the type of salts used (e.g. chlorides, sulfates, nitrates), the Fe^{2+}/Fe^{3+} ratio, the reaction temperature, the pH value and ionic strength of the media. With this synthesis, once the synthetic conditions are fixed, the quality of the magnetite nanoparticles is fully reproducible. The magnetic saturation values of magnetite nanoparticles are experimentally determined to be in the range of 30–50 emug^{-1}, which is lower than the bulk value, 90 emug^{-1}. Magnetite nanoparticles are not very stable under ambient conditions, and are easily oxidized to maghemite or dissolved in an acidic medium. Since maghemite is a ferrimagnet, oxidation is the lesser problem. Therefore, magnetite particles can

be subjected to deliberate oxidation to convert them into maghemite. This transformation is achieved by dispersing them in acidic medium, then addition of iron(III) nitrate. The maghemite particles obtained are then chemically stable in alkaline and acidic medium.

However, even if the magnetite particles are converted into maghemite after their initial formation, the experimental challenge in the synthesis of Fe_3O_4 by co-precipitation lies in control of the particle size and thus achieving a narrow particle size distribution. Since the blocking temperature depends on particle size, a wide particle size distribution will result in a wide range of blocking temperatures and therefore non-ideal magnetic behavior for many applications. Particles prepared by co-precipitation unfortunately tend to be rather polydisperse. It is well known that a short burst of nucleation and subsequent slow controlled growth is crucial to produce monodisperse particles. Controlling these processes is therefore the key in the production of monodisperse iron oxide magnetic nanoparticles.

Recently, significant advances in preparing monodisperse magnetite nanoparticles, of different sizes, have been made by the use of organic additives as stabilization and/or reducing agents. Recent studies showed that oleic acid is the best candidate for the stabilization of Fe_3O_4. The effect of organic ions on the formation of metal oxides or oxyhydroxides can be rationalized by two competing mechanisms. Chelation of the metal ions can prevent nucleation and lead to the formation of larger particles because the number of nuclei formed is small and the system is dominated by particle growth. On the other hand, the adsorption of additives on the nuclei and the growing crystals may inhibit the growth of the particles, which favors the formation of small units [1].

3.2 Thermal decomposition

Inspired by the synthesis of high-quality semiconductor nanocrystals and oxides in non-aqueous media by thermal decomposition, similar methods for the synthesis of magnetic particles with control over size and shape have been developed. Monodisperse magnetic nanocrystals with smaller size can essentially be synthesized through the thermal decomposition of organometallic compounds in high-boiling organic solvents containing stabilizing surfactants. The organometallic precursors include metal acetylacetonates, [M(acac)$_n$], (M=Fe, Mn, Co, Ni, Cr; n=2 or 3, acac=acetylacetonate), metal cupferronates [M^{x}Cup$_x$] (M=metal ion; Cup=*N*-nitrosophenylhydroxylamine, $C_6H_5N(NO)O-$), or

carbonyls. Fatty acids, oleic acid, and hexadecylamine are often used as surfactants. In principle, the ratios of the starting reagents including organometallic compounds, surfactant, and solvent are the decisive parameters for the control of the size and morphology of magnetic nanoparticles. The reaction temperature, reaction time, as well as aging period may also be crucial for the precise control of size and morphology.

If the metal in the precursor is zerovalent, such as in carbonyls, thermal decomposition initially leads to formation of the metal, but two-step procedures can be used to produce oxide nanoparticles as well. For instance, iron pentacarbonyl can be decomposed in a mixture of octyl ether and oleic acid at 100 ºC, subsequent addition of trimethylamine oxide $(CH_3)_3NO$ as a mild oxidant at elevated temperature, results in formation of monodisperse γ-Fe_2O_3 nanocrystals with a size of approximately 13 nm. Decomposition of precursors with cationic metal centers leads directly to the oxides, that is, to Fe_3O_4, if $[Fe(acac)_3]$ is decomposed in the presence of 1,2 hexadecanediol, oleylamine, and oleic acid in phenol ether. Peng and co-workers reported a general decomposition approach for the synthesis of size- and shapecontrolled magnetic oxide nanocrystals based on the pyrolysis of metal fatty acid salts in non-aqueous solution.[69] The reaction system was generally composed of the metal fatty acid salts, the corresponding fatty acids (decanoic acid, lauric acid, myristic acid, palmitic acid, oleic acid, stearic acid), a hydrocarbon solvent (octadecene (ODE), n-eicosane, tetracosane, or a mixture of ODE and tetracosane), and activation reagents. Nearly monodisperse Fe_3O_4 nanocrystals, with sizes adjustable over a wide size range (3–50 nm) could be synthesized, with controlled shapes, including dots and cubes, as representatively shown in Figure 6.
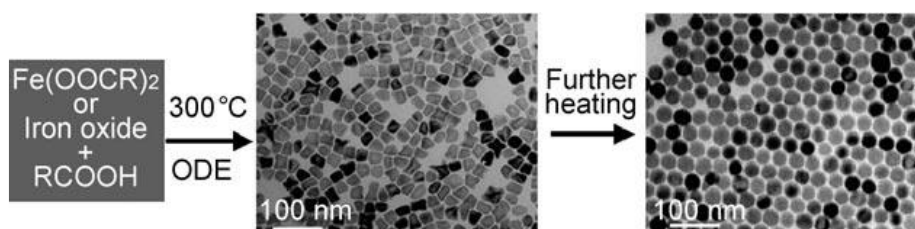

Figure 6: Monodisperse Fe₃O₄ nanocrystals

This method was successfully generalized for the synthesis of other magnetic nanocrystals, such as Cr_2O_3, MnO, Co_3O_4, and NiO. The size and shape of the nanocrystals could be controlled by variation of the reactivity and concentration of the precursors. The reactivity was tuned by changing the chain length and concentration of the fatty acids. Generally, the shorter the chain

length, the faster the reaction rate is. Alcohols or primary amines could be used to accelerate the reaction rate and lower the reaction temperature.

Hyeon and co-workers have also used a similar thermal decomposition approach for the preparation of monodisperse iron oxide nanoparticles. They used nontoxic and inexpensive iron(III) chloride and sodium oleate to generate an iron oleate complex in situ which was then decomposed at temperatures between 240 and 320ºC in different solvents, such as 1-hexadecene, octyl ether, 1-octadecene, 1-eicosene, or trioctylamine. Particle sizes are in the range of 5–22 nm, depending on the decomposition temperature and aging period. In this synthesis, aging was found to be a necessary step for the formation of iron oxide nanoparticles. The nanoparticles obtained are dispersible in various organic solvents including hexane and toluene. However, it is unclear whether the particles can also be dispersed in water. The same group found that sequential decomposition of iron pentacarbonyl and the iron oleate complex at different temperature results in the formation of monodisperse iron nanoparticles (6–15 nm) which can be further oxidized to magnetite. The overall process is similar to seed-mediated growth, which can be explained by the classical LaMer mechanism. That is, a short burst of nucleation from a supersaturated solution is followed by the slow growth of particles without any significant additional nucleation, thereby achieving a complete separation of nucleation and growth. In Hyeon's synthesis, the thermal decomposition of iron pentacarbonyl at relatively low temperature induces nucleation, and the decomposition of the iron oleate complex at a higher temperature leads to growth. The above-mentioned nanoparticles are dispersible in organic solvents. However, water soluble magnetic nanoparticles are more desirable for applications in biotechnology. For that purpose, a very simple synthesis of water-soluble magnetite nanoparticles was reported recently. Using $FeCl_3 \cdot 6H_2O$ as iron source and 2- pyrrolidone as coordinating solvent, water soluble Fe_3O_4 nanocrystals were prepared under reflux (245 ºC). The mean particles size can be controlled at 4, 12, and 60 nm, respectively, when the reflux time is 1, 10, and 24 h. With increasing reflux time, the shapes of the particles changed from spherical at early stage to cubic morphologies for longer times. More recently, the same group developed a one-pot synthesis of water-soluble magnetite nanoparticles prepared under similar reaction conditions by the addition of α, ω dicarboxyl-terminated poly(ethylene

glycol) as a surfacecapping agent. These nanoparticles can potentially be use as magnetic resonance imaging contrast agents for cancer diagnosis.

The thermal-decomposition method is also used to prepare metallic nanoparticles. The advantage of metallic nanoparticles is their larger magnetization compared to metal oxides, which is especially interesting for data-storage media. Metallic iron nanoparticles were synthesized by thermal decomposition of $[Fe(CO)_5]$ and in the presence of polyisobutene in decalin under nitrogen atmosphere at 170ºC. The particle size can be adjusted from 2 to 10 nm, with a polydispersity of approximately 10%, depending on the ratio of $Fe(CO)_5$/polyisobutene. The thickness of the polymer layer around the iron nanoparticles was about 7.0 nm. However, these iron particles can still be easily oxidized by exposure to air, as revealed by the susceptibility measurements. This leads to a slight increase of particle sizes by a factor of approximately 1.3. Chaudret and co-workers reported a synthesis of iron nanocubes by the decomposition of $[Fe\{N[Si(CH_3)_3]_2\}_2]$ with H_2 in the presence of hexadecylamine and oleic acid or hexadecylammonium chloride at 150 ºC. By variation of the relative concentrations of amine and acid ligand, the size (edge-length) of the nanocubes can be slightly varied from 7 to 8.3 nm with the interparticle space of 1.6nm to 2 nm, respectively. These nanocubes can assemble into extended crystalline superlattices with their crystallographic axes aligned.

In the synthesis of cobalt nanoparticles by the thermal-decomposition method, both their shape and size can be controlled. Alivisatos and co-workers reported the synthesis of cobalt nanodisks by the thermal decomposition of a cobalt carbonyl precursor. Chaudret and co-workers described the synthesis of cobalt nanorods and nickel nanorods from the high-temperature reduction of noncarbonyl organometallic complexes. For instance, monodisperse ferromagnetic cobalt nanorods were synthesized through the decomposition of $[Co(\eta_3\text{-}C_8H_{13})(\eta_4\text{-}C_8H_{12})]$ under H_2 in anisole at 150ºC in the presence of a mixture of hexadecylamine and a fatty acid, such as lauric acid, octanoic acid, or

stearic acid. As seen in Figure 3, the diameter and length of the cobalt nanorods are variable by selecting different acids.

Air-stable magnetic nanoparticles are very attractive in terms of easy handling and application under oxidizing conditions. Bönnemann et al. reported the synthesis of air-stable "monodisperse" colloidal cobalt nanoparticles by the thermolysis of $[Co_2(CO)_8]$ in the presence of aluminum alkyl compounds. By varying the alkyl chain length of the organo aluminum compounds, the sizes of the Co particles can be tuned in the range of 3–11 nm. It was found that gentle surface oxidation of the cobalt nanoparticles with synthetic air was necessary and
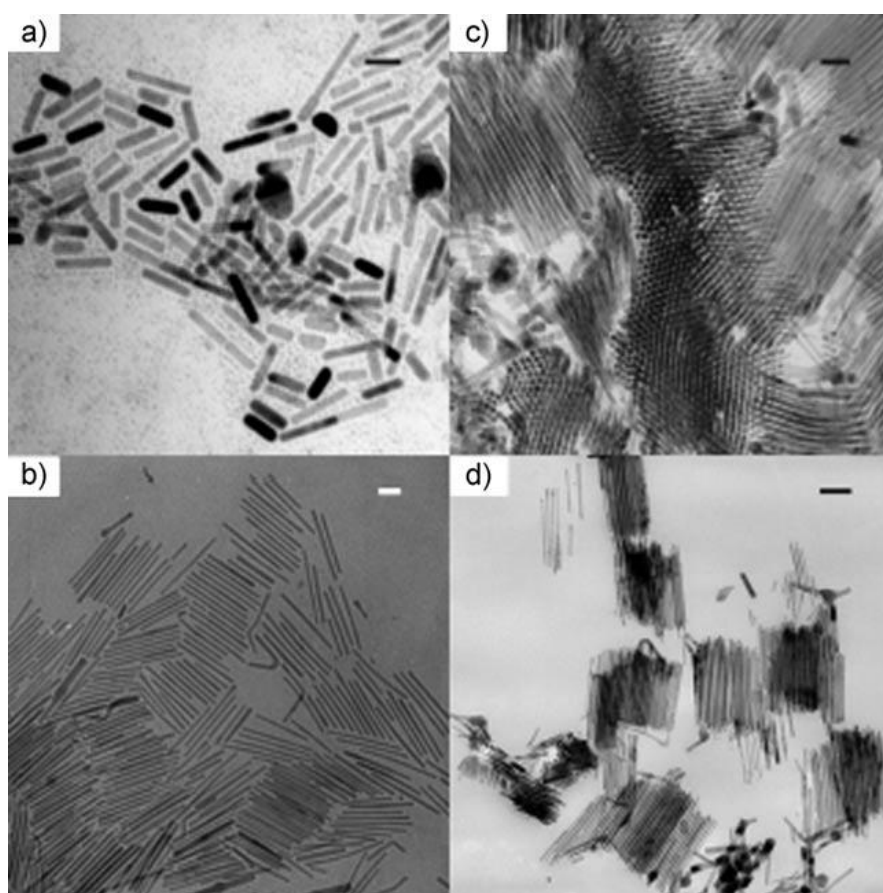
Figure 7: TEM micrographs of nanorods synthesized using hexadecylamine and a) octanoic acid, b) lauric acid, and c, d) stearic acid.

crucial to obtain air-stable particles. Without this oxidation step, saturation magnetization of the Co^0 particles decays rapidly when exposed to air after the peptization with the surfactant KorantinSH.

Magnetic alloys have many advantages, such as high magnetic anisotropy, enhanced magnetic susceptibility, and large coercivities. Beside $CoPt_3$ and FePt, metal phosphides are currently of great scientific interest in materials science and chemistry. For example, hexagonal iron phosphide and related materials have

been intensively studied for their ferromagnetism, magnetoresistance, and magnetocaloric effects. Recently, Brock and co-workers have synthesized FeP and MnP nanoparticles from the reaction of iron(III) acetylacetonate and manganese carbonyl, respectively, with tris(trimethylsilyl)phosphane at high temperatures. Very recently, antiferromagnetic FeP nanorods were prepared by the thermal decomposition of a precursor/surfactant mixture solution. In addition, synthesis of discrete iron phosphide (Fe_2P) nanorods from the thermal decomposition of continuously supplied iron pentacarbonyl in trioctylphosphane using a syringe pump was reported [1].

3.3 Microemulsion

A microemulsion is a thermodynamically stable isotropic dispersion of two immiscible liquids, where the microdomain of either or both liquids is stabilized by an interfacial film of surfactant molecules. In water-in-oil microemulsions, the aqueous phase is dispersed as microdroplets (typically 1– 50 nm in diameter) surrounded by a monolayer of surfactant molecules in the continuous hydrocarbon phase. The size of the reverse micelle is determined by the molar ratio of water to surfactant. By mixing two identical water-in-oil microemulsions containing the desired reactants, the microdroplets will continuously collide, coalesce, and break again, and finally a precipitate forms in the micelles. By the addition of solvent, such as acetone or ethanol, to the microemulsions, the precipitate can be extracted by filtering or centrifuging the mixture. In this sense, a microemulsion can be used as a nanoreactor for the formation of nanoparticles.

Using the microemulsion technique, metallic cobalt, cobalt/platinum alloys, and gold-coated cobalt/platinum nanoparticles have been synthesized in reverse micelles of cetyltrimethlyammonium bromide, using 1-butanol as the cosurfactant and octane as the oil phase. MFe_2O_4 (M: Mn, Co, Ni, Cu, Zn, Mg, or Cd, etc.) are among the most important magnetic materials and have been widely used for electronic applications. Spinel ferrites can be synthesized in microemulsions and inverse micelles. For instance, $MnFe_2O_4$ nanoparticles with controllable sizes from about 4–15 nm are synthesized through the formation of water-in-toluene inverse micelles with sodium dodecylbenzenesulfonate (NaDBS) as surfactant. This synthesis starts with a clear aqueous solution consisting of $Mn(NO_3)_2$ and $Fe(NO_3)_3$. A NaDBS aqueous solution is added to the metal salt solution, subsequent addition of a large volume of toluene forms reverse micelles. The volume ratio of water and toluene determines the size of the resulting $MnFe_2O_4$

nanoparticles. Woo et al. reported that iron oxide nanorods can be fabricated through a sol–gel reaction in reverse micelles formed from oleic acid and benzyl ether, using $FeCl_3 \cdot 6H_2O$ as iron source and propylene oxide as a proton scavenger. The phase of the nanorods can be controlled by variation of the reaction temperature, atmosphere, and hydration state of the gels during reflux or heating in tetralin. A cobalt ferrite fluid was prepared by the reaction of methylamine and in-situ formed cobalt and iron dodecyl sulfate which were made by mixing an aqueous solution of sodium dodecyl sulfate either with iron chloride or with cobalt acetate solution. The size of the cobalt ferrite particles decreases with decreasing total reactant concentration and increasing sodium dodecyl sulfate concentration. The average size of the particles can be varied from 2 to 5 nm. However, the polydispersity is rather high at 30–35%.

Using the microemulsion technique, nanoparticles can be prepared as spheroids, but also with an oblong cross section or as tubes. Although many types of magnetic nanoparticles have been synthesized in a controlled manner using the microemulsion method, the particle size and shapes usually vary over a relative wide range. Moreover, the working window for the synthesis in microemulsions is usually quite narrow and the yield of nanoparticles is low compared to other methods, such as thermal decomposition and coprecipitation. Large amounts of solvent are necessary to synthesize appreciable amounts of material. It is thus not a very efficient process and also rather difficult to scale-up [1].

3.4 Hydrothermal Synthesis

Under hydrothermal conditions a broad range of nanostructured materials can be formed. Li et al. reported a generalized hydrothermal method for synthesizing a variety of different nanocrystals by a liquid–solid–solution reaction. The system consists of metal linoleate (solid), an ethanol– linoleic acid liquid phase, and a water–ethanol solution at different reaction temperatures under hydrothermal conditions. As illustrated in Figure 8, this strategy is based on a general phase transfer and separation mechanism occurring at the interfaces of the liquid, solid, and solution phases present during the synthesis. As an example, Fe_3O_4 and $CoFe_2O_4$ nanoparticles can be prepared in very uniform sizes of about 9 and 12 nm, respectively (see Figure 8). Li et al. also reported a synthesis of monodisperse, hydrophilic, singlecrystalline ferrite microspheres by hydrothermal reduction. A mixture, consisting of $FeCl_3$, ethylene glycol, sodium

acetate, and polyethylene glycol, was stirred vigorously to form a clear solution, then sealed in a Teflon-lined stainless-steel autoclave, and heated to and maintained at 200 °C for 8–72 h. In this way, monodisperse ferrite spheres were obtained with tunable sizes in the range of 200–800 nm. Li et al. skillfully used the multicomponent reaction mixtures, including ethylene glycol, sodium acetate, and polyethylene glycol, to direct the synthesis: Ethylene glycol was used as a high-boiling-point reducing agent, which was known from the polyol process to produce monodisperse metal or metal oxide nanoparticles; sodium acetate as electrostatic stabilizer to prevent particle agglomeration, and polyethylene glycol as a surfactant against particle agglomeration.

Although the mechanism is not fully clear to date, the multicomponent approach seems to be powerful in directing the formation of desired materials.
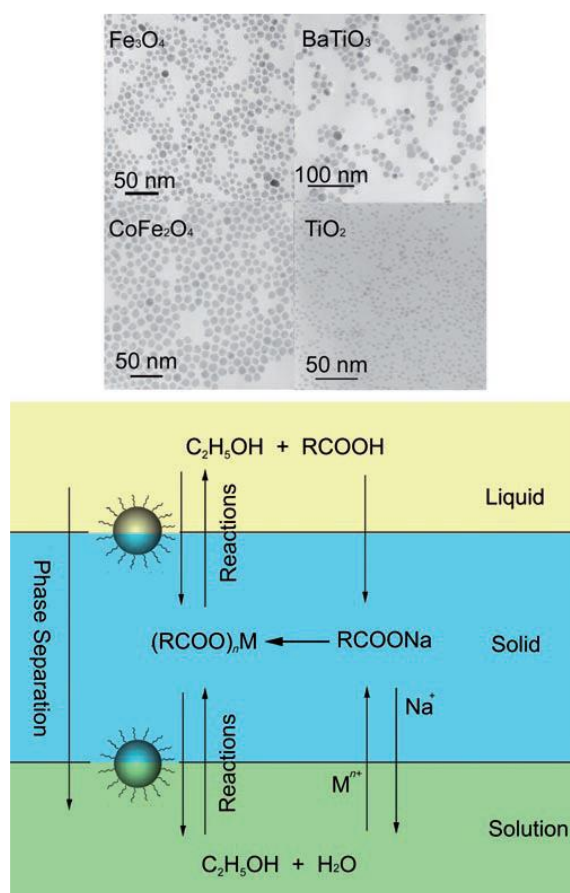

Figure 8: Top: TEM images of Magnetic and dielectric nanocrystals: Fe_3O_4 (9.1 nm), $CoFe_2O_4$ (11.5 nm;), $BaTiO_3$ (16.8 nm;), TiO_2 (4.3 nm). Bottom: The liquid-solid-solution (LSS) phasetransfer synthetic strategy.

The advantages and disadvantages of the four abovementioned synthetic methods are briefly summarized in Table 3. In terms of simplicity of the synthesis,

co-precipitation is the preferred route. In terms of size and morphology control of the nanoparticles, thermal decomposition seems the best method developed to date. As an alternative, microemulsions can also be used to synthesize monodispersed nanoparticles with various morphologies. However, this method requires a large amount of solvent. Hydrothermal synthesis is a relatively little explored method for the synthesis of magnetic nanoparticles, although it allows the synthesis of high-quality nanoparticles. To date, magnetic nanoparticles prepared from co-precipitation and thermal decomposition are the best studied, and they can be prepared on a large scale.

The colloidal stability of magnetic nanoparticles synthesized by the above-mentioned methods results either from steric or electrostatic repulsion, depending on the stabilizers, such as fatty acids or amines, and the polarity of the solvent used. For instance, magnetite nanoparticles synthesized through co-precipitation were stabilized by repulsive electrostatic forces because the particles are positively charged. However, nanoparticles synthesized by thermal decomposition are, in general, sterically stabilized in an organic solvent by fatty acids or surfactant. In the following section, the colloidal and chemical stability will be discussed [1].

4 Protection and stabilization of magnetic nanoparticles

It is necessary to develop efficient strategies to improve the chemical stability of magnetic nanoparticles. The most straightforward method seems to be protection by a layer which is impenetrable, so that oxygen can not reach the surface of the magnetic particles. Often, stabilization and protection of the particles are closely linked with each other

4.1 Surfactant and Polymer Coating

Surfactants or polymers are often employed to passivate the surface of the nanoparticles during or after the synthesis to avoid agglomeration. In general, electrostatic repulsion or steric repulsion can be used to disperse nanoparticles and keep them in a stable colloidal state. The best known example for such systems are the ferrofluids which were invented by Papell in 1965. In the case of ferrofluids, the surface properties of the magnetic particles are the main factors determining colloidal stability. The major measures used to enhance the stability

of ferrofluids are the control of surface charge and the use of specific surfactants. For instance, magnetite nanoparticles synthesized through the co-precipitation of Fe^{2+} and Fe^{3+} in ammonia or NaOH solution are usually negatively charged, resulting in agglomeration. To achieve stable colloids, the magnetite nanoparticle precipitate can be peptized (to disperse a precipitate to form a colloid by adding of surfactant) with aqueous tetramethylammonium hydroxide or with aqueous perchloric acid. The magnetite nanoparticles can be acidified with a solution of nitric acid and then further oxidized to maghemite by iron nitrate. After centrifugation and redispersion in water, a ferrofluid based on positively charged γ-Fe_2O_3 nanoparticles was obtained, since the surface hydroxy groups are protonated in the acidic medium. Commercially, water- or oilbased ferrofluids are available. They are usually stable when the pH value is below 5 (acidic ferrofluid) or over 8 (alkalin ferrofluid).

In general, surfactants or polymers can be chemically anchored or physically adsorbed on magnetic nanoparticles to form a single or double layer, which creates repulsive (mainly as steric repulsion) forces to balance the magnetic and the van der Waals attractive forces acting on the nanoparticles. Thus, by steric repulsion, the magnetic particles are stabilized in suspension. Polymers containing functional groups, such as carboxylic acids, phosphates, and sulfates, can bind to the surface of magnetite. Suitable polymers for coating include poly(pyrrole), poly(aniline), poly(alkylcyanoacrylates), poly(methylidene malonate), and polyesters, such as poly(lactic acid), poly (glycolic acid), poly(e-caprolactone), and their copolymers. Surface-modified magnetic nanoparticles with certain biocompatible polymers are intensively studied for magnetic-field-directed drug targeting, and as contrast agents for magnetic resonance imaging.

Chu et al. reported a synthesis of polymer-coated magnetite nanoparticles by a single inverse microemulsion. The magnetite particles were first synthesized in an inverse microemulsion, consisting of water/sodium bis(2-ethylhexylsulfosuccinate)/ toluene. Subsequently, water, monomers (methacrylic acid and hydroxyethyl methacrylate), crosslinker (N,N'-methylenebis(acrylamide)), and an initiator (2,2'-azobis(isobutyronitrile)) were added to the reaction mixture under nitrogen, and the polymerization reaction was conducted at 55ºC. After polymerization, the particles were recovered by precipitation in an excess of an acetone/ methanol mixture (9:1 ratio). The polymer-coated nanoparticles have superparamagnetic properties and a narrow

size distribution at a size of about 80 nm. However, the longterm stability of these polymer-coated nanoparticles was not addressed. Polyaniline can also be used to coat nanosized ferromagnetic Fe_3O_4 by oxidative polymerization in the presence of the oxidant ammonium peroxodisulfate. The nanoparticles obtained are polydisperse (20–30 nm averaged diameter) and have the expected core–shell morphology. Asher et al. reported that single iron oxide particles (ca. 10 nm) can be embedded in polystyrene spheres through emulsion polymerization to give stable superparamagnetic photonic crystals. Polystyrene coating of iron oxide nanoparticles was also achieved by atom transfer radical polymerization. For instance, Zhang et al. have used this method for coating $MnFe_2O_4$ nanoparticles with polystyrene, yielding core–shell nanoparticles with sizes below 15 nm. The overall synthetic procedure is schematically shown in Figure 9. $MnFe_2O_4$ nanoparticles (ca. 9 nm) were stirred overnight in aqueous initiator solution, 3-chloropropionic acid, at pH 4. After washing out the excess initiator, air-dried nanoparticles were added to a styrene solution under nitrogen, then
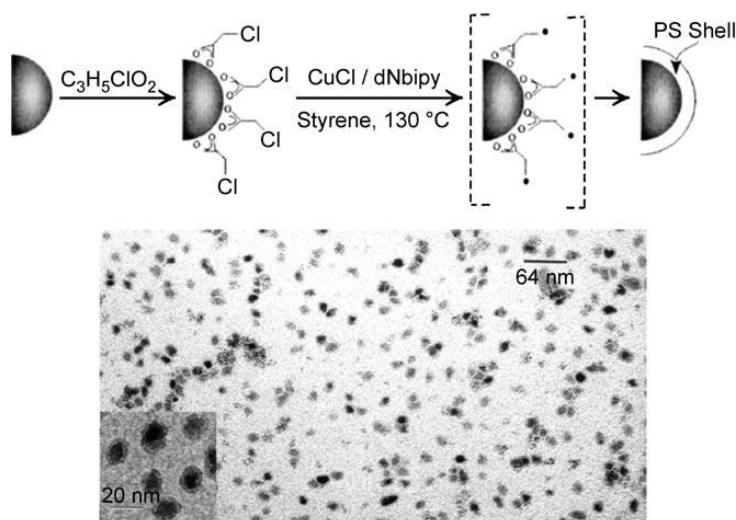

Figure 9: Top: Illustration of the polystyrene coating on MnFe2O4 by atom-transfer radical polymerization. Bottom: TEM micrographs of approximately 9-nm diameter MnFe2O4/polystyrene core–shell nanoparticles.

xylene, containing CuCl and 4,4'-dinonyl-2,2'-dipyridyl was added. The solution was stirred and kept at 130ºC for 24 h to give the polystyrene coated $MnFe_2O_4$ nanoparticles. When using a free radical polymerization with $K_2S_2O_8$ as the catalyst, predominantly polystyrene particles without a magnetic core were obtained. This result confirms that the surface-grafted initiator is important for the coating of the nanoparticles.

Metallic magnetic nanoparticles, stabilized by single ordouble layers of surfactant or polymer are not air stable, and are easily leached by acidic solution, resulting in the loss of their magnetization. A thin polymer coating is not a good enough barrier to prevent oxidation of the highly reactive metal particles. Polymer coating is thus not very suitable to protect very reactive magnetic nanoparticles.

Another drawback of polymer-coated magnetic nanoparticles is the relatively low intrinsic stability of the coating at higher temperature, a problem which is even enhanced by a possible catalytic action of the metallic cores. Therefore, the development of other methods for protecting magnetic nanoparticles against deterioration is of great importance [1].

4.2 Precious-Metal Coating

Precious metals can be deposited on magnetic nanoparticles through reactions in microemulsion, redox transmetalation, iterative hydroxylamine seeding, or other methods, to protect the cores against oxidation. Cheon et al. reported a synthesis of platinum-coated cobalt by refluxing cobalt nanoparticle colloids (ca. 6nm) and [Pt- (hfac)$_2$] (hfac=hexafluoroacetylacetonate) in a nonane solution containing $C_{12}H_{25}NC$ as a stabilizer. After 8 h reflux and addition of ethanol and centrifugation, the colloids are isolated from the dark red-black solution in powder form. The TEM images of the platinum-coated cobalt particles with sizes below 10 nm are shown in Figure 10.
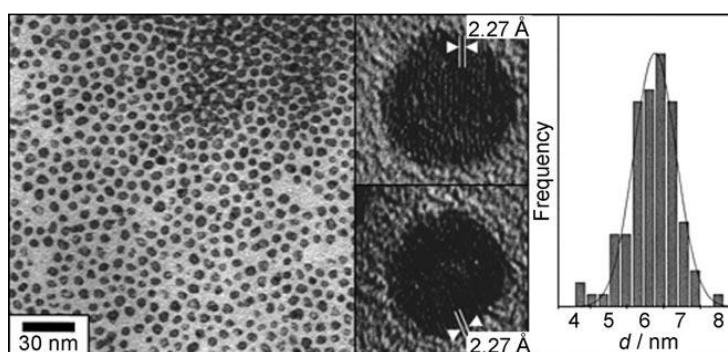

Figure 10: Left: TEM images of CocorePtshell nanoalloys. In the enlarged images the spacings of the lattice fringes are given which are consistent with the Pt(111) plane. Right: the particle size distribution.

These particles are air stable and can be redispersed in typical organic solvents. The reaction byproduct was separated and analyzed as [Co(hfac)$_2$], indicating that the formation of the core–shell structure was driven by redox transmetalation reactions between Co^0 and Pt^{2+}.

Gold seems to be an ideal coating owing to its low reactivity. However, it was found that the direct coating of magnetic particles with gold is very difficult, because of the dissimilar nature of the two surfaces. Progress has been made, though, recently. O'Connor and co-workers have synthesized gold-coated iron nanoparticles with about 11 nm core size and a gold shell of about 2.5 nm thickness. These golds coated iron particles are stable under neutral and acidic aqueous conditions. The coating was achieved by a partial replacement reaction in a polar aprotic solvent. Briefly, a yellow solution of $FeCl_3$, dissolved in 1-methyl-2- pyrrolidinone (NMPO), was added to a dark green NMPO solution containing sodium and naphthalene under intensive stirring at room temperature. Thus, the Fe^{3+} ions were reduced by sodium to form the metallic cores. After removal of sodium chloride by centrifugation, and the addition of 4- benzylpyridine as capping agent at elevated temperature, the iron nanoparticles were coated with gold by the addition of dehydrated $HAuCl_4$ dissolved in NMPO.

Gold-coated iron nanoparticles could also be prepared by a reverse microemulsion method. The inverse micelles were formed with cetyltrimethylammonium bromide (CTAB) as surfactant, 1-butanol as a co-surfactant, and octane as the continuous oil phase. $FeSO_4$ was reduced by $NaBH_4$, then addition of $HAuCl_4$ coated gold on the iron nanoparticles. Zhang et al. reported a new method for the preparation of gold coated iron magnetic core–shell nanoparticles by the combination of wet chemistry and laser irradiation. The synthesized iron nanoparticles and gold powder were irradiated by a laser in a liquid medium to deposit the gold shell. The 18 nm body centered cubic (bcc) iron single domain magnetic cores are covered by a gold shell of partially fused approximately 3-nm-diameter fcc gold nanoparticles. The core–shell particles are superparamagnetic at room temperature with a blocking temperature, T_B, of approximately 170 K. After four months of shelf storage in normal laboratory
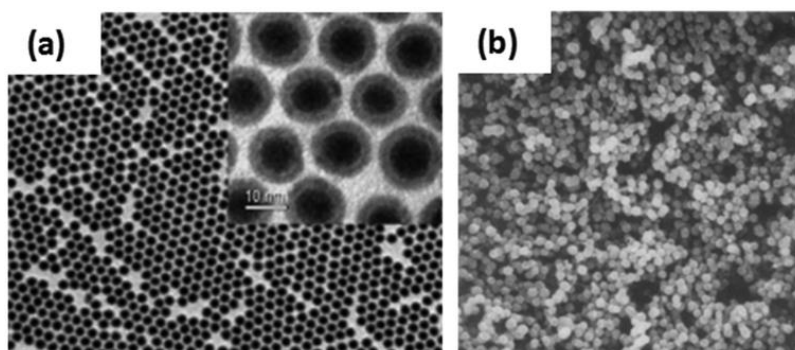

Figure 11: (a)TEM image of 4 nm/2.5 nm Fe/Fe$_3$O$_4$
nanoparticles; (b) SEM image of Fe3O4 nanoparticles.

conditions, their magnetization normalized to iron content was measured to be 210 emug^{-1}, roughly 96% of the bulk iron value, which indicates the high stability.

Guo et al. have reported a synthesis of gold coated cobalt nanoparticles based on a chemical reduction reaction. The cobalt particles were fabricated using 3-(*N,N*-dimethyldodecylammonio) propanesulfonate as the surfactant to prevent agglomeration, and lithium triethylhydridoborate as the reducing agent. The cobalt nanoparticles produced were added to KAuCl$_4$ in tetrahydrofuran (THF) solution under ultrasonication and inert atmosphere. The gold shell was deposited on the cobalt nanoparticle through reduction of the Au^{3+} by cobalt surface atoms.

Gold coating of magnetic nanoparticles is especially interesting, since the gold surface can be further functionalized with thiol groups. This treatment allows the linkage of functional ligands which may make the materials suitable for catalytic and optical applications [1].

4.3 Silica Coating

A silica shell does not only protect the magnetic cores, but can also prevent the direct contact of the magnetic core with additional agents linked to the silica surface thus avoiding unwanted interactions. For instance, the direct attachment of dye molecules to magnetic nanoparticles often results in luminescence quenching. To avoid this problem, a silica shell was first coated on the magnetic core, and then dye molecules were grafted on the silica shell. Silica coatings have several advantages arising from their stability under aqueous conditions (at least if the pH value is sufficiently low), easy surface modification, and easy control of interparticle interactions, both in solution and within structures, through variation of the shell thickness.

The Stöber method and sol–gel processes are the prevailing choices for coating magnetic nanoparticles with silica. The coating thickness can be tuned by varying the concentration of ammonium and the ratio of tetraethoxysilane (TEOS) to H$_2$O. The surfaces of silica-coated magnetic nanoparticles are hydrophilic, and are readily modified with other functional groups. The functionalization could introduce additional functionality, so that the magnetic particles are potentially of use in biolabeling, drug targeting, drug delivery. Previous studies involved the coating of hematite (Fe$_2$O$_3$) spindles and much smaller magnetite clusters with silica; the oxide cores could subsequently be

reduced in the dry state to metallic iron. The advantage of this method is that silica coating was performed on an oxide surface, which easily binds to silica through OH surface groups.
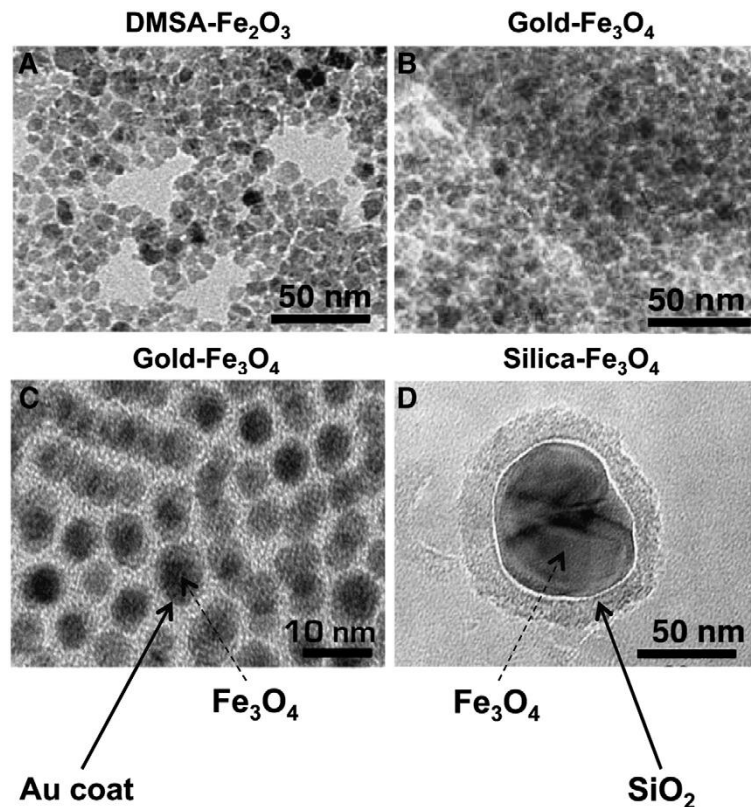

Figure 12: TEM image from Gold and Silica coatings.

Xia and co-workers have shown that commercially available ferrofluids can be directly coated with silica shells by the hydrolysis of TEOS. A water-based ferrofluid (EMG 340) was diluted with deionized water and 2-propanol. Ammonia solution and various amounts of TEOS were added stepwise to the reaction mixture under stirring. The coating step was allowed to proceed at room temperature for about 3 h under continuous stirring. The coating thickness could be varied by changing the amount of TEOS. Since the iron oxide surface has a strong affinity towards silica, no primer was required to promote the deposition and adhesion of silica. Owing to the negative charges on the silica shells, these coated magnetic nanoparticles are redispersible in water without the need of adding other surfactants. Figure 7 shows the TEM images of silica-coated iron oxide nanoparticles. The images clearly indicate the single-crystalline nature of the iron oxide core and the amorphous nature of the silica shell. Kobayashi et al. described a method for the synthesis of monodisperse, amorphous cobalt nanoparticles coated with silica in aqueous ethanolic solution by using 3-

aminopropyl trimethoxysilane and TEOS as the silica precursor. Shi and co-workers have prepared uniform magnetic nanospheres (ca. 270 nm) with a magnetic core and a mesoporous-silica shell. The synthesis involved forming a thin and dense silica coating on hematite nanoparticles by the StPber process, a second coating, the mesoporous silica shell, was added by a simultaneous sol–gel polymerization of TEOS and n-octadecyltrimethoxysilane. The hematite core can be reduced to the metallic state by H_2.
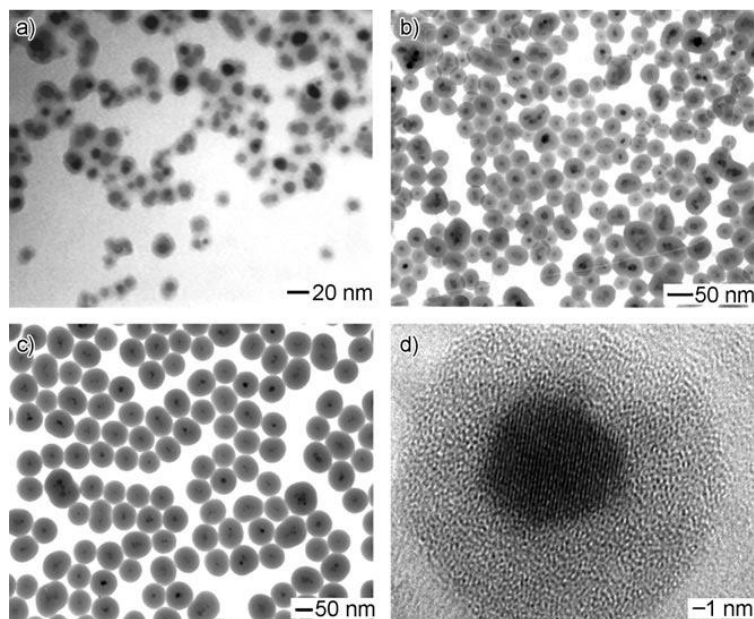
Figure 13: Silica coated NMPs

Though great progress in the field of silica-coated nanoparticles has been made, the synthesis of uniform silica shells with controlled thickness on the nanometer scale still remains challenging. As an alternative, the microemulsion method was also tried. Homogeneous silica-coated Fe_2O_3 nanoparticles with a silica shell of controlled thickness (1.8–30 nm) were synthesized in a reverse microemulsion. Tartaj et al. reported a synthesis of monodisperse air-stable superparamagnetic α-Fe nanocrystals encapsulated in nanospherical silica particles of 50 nm in diameter. The iron oxide nanoparticles are embedded in silica by the reverse microemulsion technique, the a-Fe is obtained by reduction with hydrogen at 450 °C. Similarly, a reverse micelle microemulsion approach was also reported to coat a layer of silica around spinel ferrite nanoparticles of $CoFe_2O_4$ and $MnFe_2O_4$.

Although metals protected by silica can be synthesized by reduction after synthesis, silica deposition directly on pure metal particles is more complicated because of the lack of OH groups on the metal surface. An additional difficulty for coating metallic nanoparticles, such as iron and cobalt with silica, which has to be overcome, is that iron and cobalt are readily oxidized in the presence of dissolved oxygen. Therefore, it is necessary to use a primer to make the surface "vitreophilic" (glasslike). This chemistry has been used to coat precious metals. Another possibility would be using stable cobalt nanoparticles, passivated by the gentle oxidation method developed by BPnnemann et al., as starting materials for such silica coating. However, no corresponding report has appeared to date.

Other oxides have rarely been used as protective coatings. Needlelike yttria-coated FeCo nanoparticles were synthesized starting from needlelike YCo-FeOOH nanoparticles, by the combination of a modified carbonate route and electrostatically induced self-assembly methods. The use of yttria as a protective agent has allowed the dehydration temperature of the oxyhydroxides to be increased, decreasing the porosity of samples, and thus improving the magnetic properties of the final metallic particles. The highest value of coercivity (1550 Oe) is obtained for samples containing 20 mol% of cobalt.

From the mentioned examples above, it can be seen that silica coating of magnetic oxide nanoparticles is a fairly controllable process. However, silica is unstable under basic condition, in addition, silica may contain pores through which oxygen or other species could diffuse. Coating with other oxides is much less developed, and therefore alternative methods, especially those which would allow stabilization under alkaline conditions, are needed [1].

4.4 Carbon coating

Although to date most studies have focused on the development of polymer or silica protective coatings, recently carbon-protected magnetic nanoparticles are receiving more attention, because carbon-based materials have many advantages over polymer or silica, such as much higher chemical and thermal stability as well as biocompatibility.

Right after the discovery of fullerenes, it was found that carbon-encapsulated metal or metal carbide nanocrystallites can be generated by the KrStschmer arc-discharge process. Since then, many studies have shown that in the presence of metal nanoparticles (Co, Fe, Ni, Cr, Au, etc), graphitized carbon structures, such

as carbon nanotubes and carbon onions, are formed under arc-discharge, laser ablation, and electron irradiation. The well-developed graphitic carbon layers provide an effective barrier against oxidation and acid erosion. These facts indicate that it is possible to synthesize carbon-coated magnetic nanoparticles, which are thermally stabile and have high stability against oxidation and acid leaching, which is crucial for some applications. Moreover, carbon-coated nanoparticles are usually in the metallic state, and thus have a higher magnetic moment than the corresponding oxides.

Gedanken and co-workers reported a sonochemical procedure that leads to air-stable cobalt nanoparticles. They claim that the high stability arises from the formation of a carbon shell on the nanoparticle surface. However, the particles obtained are rather polydisperse and not very uniform. Johnson et al. describe a simple method to prepare carbon-coated magnetic Fe and Fe_3C nanoparticles by direct pyrolysis of iron stearate at 900ºC under an argon atmosphere. The carbon-coated magnetic nanoparticles obtained are stable up to 400ºC under air. This direct salt-conversion process is an advantageous single-step process and potentially can be scaled up. However, the nanoparticles produced by this method show a broad size distribution, with a diameter ranging from 20 to 200 nm and the cores are covered with 20 to 80 graphene layers. No information on dispersibility of the nanoparticles was given. Lu et al. have synthesized highly stable carbon-coated cobalt nanoparticles with a size of about 11 nm. The cobalt nanoparticles were coated with furfurly alcohol which was converted first into poly (furfuryl alcohol) and then carbonized to carbon during the pyrolysis, resulting in a stable protection layer against air oxidation, and erosion by strong acids and bases. Interestingly, if CTAB is used as the carbon source, the carbon coating is not perfect and the cobalt core can be leached with acid. Since the imperfect graphite coating is not attacked, graphitic hollow shells were obtained, which may be interesting for use as electrodes. Similar graphitic-carbon-encapsulated cobalt nanoparticles were also prepared through pyrolysis of a composite of metallic cobalt nanoparticles (ca. 8–10 nm) and poly(styrene-*b*-4-vinylphenoxyphthalonitrile). These cobalt-graphitic particles are oxidatively stable and retain their high saturation magnetizations (ca. 95–100 emug[-1]) for at least one year under ambient conditions.

We have recently investigated the structure development of cobalt cations chemically adsorbed in an in-house synthesized ion-exchangeable polymer.

During pyrolysis, the in-situ formed cobalt nanoparticles continuously catalyze the decomposition of the polymer matrix to form mesoporous graphitic carbon. Cobalt nanoparticles embedded in graphitic carbon were obtained as the final product. Magnetization measurements show that the graphitic carbon/cobalt composites are ferromagnetic, and the cobalt nanoparticles are stable under air for more than 10 months without degradation of their magnetic properties.

Though carbon-coated magnetic nanoparticles have many advantageous properties, such particles are often obtained as agglomerated clusters, owing to the lack of effective synthetic methods, and a low degree of understanding of the formation mechanism. The synthesis of dispersible, carbon-coated nanoparticles in isolated form is currently one of the challenges in this field.

5 Applications in medicine

A wide variety of potential applications have been envisaged. Since magnetic nanoparticles are expensive to produce, there is interest in their recycling or for their highly specialized applications. They are only used in scientific research. An industrial use has yet to be established.

The potential and versatility of magnetic chemistry arises from the fast and easy separation of the magnetic nanoparticles, eliminating tedious and costly separation processes usually applied in chemistry. Furthermore, the magnetic nanoparticles can be guided via a magnetic field to the desired location which could, for example, enable pinpoint precision in fighting cancer [2].

5.1 Medical diagnostics and treatments

Magnetic nanoparticles have been examined for use in an experimental cancer treatment called magnetic hyperthermia in which an alternating magnetic field (AMF) is used to heat the nanoparticles.

Affinity ligands such as epidermal growth factor (EGF), folic acid, aptamers, lectins etc. can be attached to the magnetic nanoparticle surface with the use of various chemistries. This enables targeting of magnetic nanoparticles to specific tissues or cells. This strategy is used in cancer research to target and treat tumors in combination with magnetic hyperthermia or nanoparticle-delivered cancer drugs. Despite research efforts, however, the accumulation of nanoparticles inside of cancer tumors of all types is sub-optimal, even with affinity ligands. The challenge of accumulating large amounts of nanoparticles inside of tumors is

arguably the biggest obstacle facing nanomedicine in general. While direct injection is used in some cases, intravenous injection is most often preferred to obtain a good distribution of particles throughout the tumor. Magnetic nanoparticles have a distinct advantage in that they can accumulate in desired regions via magnetically guided delivery, although this technique still needs further development to achieve optimal delivery to solid tumors.

Another potential treatment of cancer includes attaching magnetic nanoparticles to free-floating cancer cells, allowing them to be captured and carried out of the body. The treatment has been tested in the laboratory on mice and will be looked at in survival studies.

Magnetic nanoparticles can be used for the detection of cancer. Blood can be inserted onto a microfluidic chip with magnetic nanoparticles in it. These magnetic nanoparticles are trapped inside due to an externally applied magnetic field as the blood is free to flow through. The magnetic nanoparticles are coated with antibodies targeting cancer cells or proteins. The magnetic nanoparticles can be recovered and the attached cancer-associated molecules can be assayed to test for their existence [2].

Magnetic nanoparticles can be conjugated with carbohydrates and used for detection of bacteria. Iron oxide particles have been used for the detection of Gram negative bacteria like *Escherichia coli* and for detection of Gram positive bacteria like *Streptococcus suis*.

5.2 MNPs for theragnostic platforms

Theragnostics (the fusion of therapeutic and diagnostic approaches) aims to personalize and advance medicine. MNPs represent a particularly appropriate tool based on their ability to be simultaneously functionalized and guided by an external magnetic field. Novel designs have focused on sophisticated multilayering of MNPs with the goal to develop controlled nanodelivery systems. Already, functionalized MNPs have been used in combination theragnostic approaches for gene delivery with selective tumor imaging, MRI-guided therapeutic cell replacement and MRI-assisted diagnosis and surgeries using a single MNP formulation. After removal of the magnetic field MNPs do not retain magnetism, providing additional versatility. We here touch upon MNP-based therapeutic applications (e.g., magnetic hyperthermia, drug/gene delivery and tissues engineering) and diagnostic imaging or biosensor platforms, depicting

integrative approaches that capitalize on the MNPs' dual magnetic and functionalization modalities [18].

5.3 Magnetic hyperthermia

Hyperthermia is a cancer therapy that relies on the localized heating of tumors above 43 °C for about 30 min. MNPs can generate heat under alternating magnetic fields due to energy losses in the traversing of the magnetic hysteresis loop. Generation of different degrees of heat depends on the magnetization properties of specific MNP formulations and magnetic field parameters. Selectivity to tumors was considerably improved through the use of silane coatings and through functionalization approaches. For example, MNPs conjugated with antibodies to cancer-specific antigens improved selectivity of MNP uptake by tumors during hyperthermia therapy. Magnetic hyperthermia using magnetic cationic liposomes has been used in a combination approach withTNF-α gene therapy and stress-inducible gadd153 promoter, resulting in a dramatic arrest in tumor growth [18].
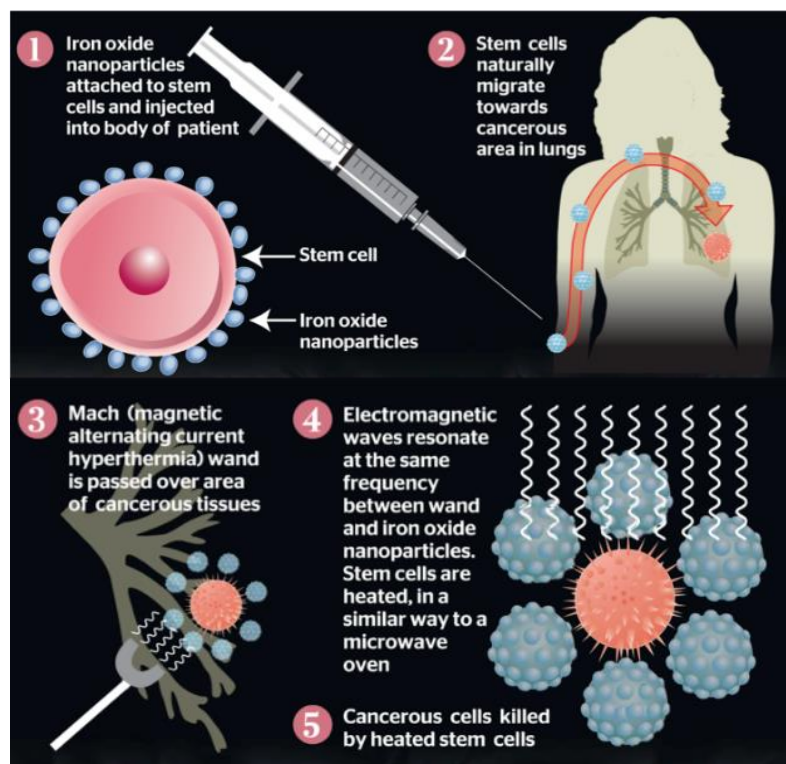

Figure 14: Process of magnetic hyperthermia in cancer treatment.

N magnetic fluid hyperthermia, nanoparticles of different types like Iron oxide, magnetite, maghemite or even gold are injected in tumor and then subjected under a high frequency magnetic field. These nanoparticles produce heat that

typically increases tumor temperature to 40-46°C, which can kill cancer cells. Another major potential of magnetic nanoparticles is the ability to combine heat (hyperthermia) and drug release for a cancer treatment. Numerous studies have shown particle constructs that can be loaded with a drug cargo and magnetic nanoparticles. The most prevalent construct is the "Magnetoliposome", which is a liposome with magnetic nanoparticles typically embedded in the lipid bilayer. Under an alternating magnetic field, the magnetic nanoparticles are heated, and this heat permeabilizes the membrane. This causes release of the loaded drug. This treatment option has a lot of potential as the combination of hyperthermia and drug release is likely to treat tumors better than either option alone, but it is still under development [2].

5.4 Magnetic resonance imaging (MRI)

MNP-enhanced MRI is based on the superior superparamagnetic qualities of iron oxide MNPs. Several dextran-coated MNP formulations have been approved for clinical use as MRI contrast agents, including ferumoxides, ferumoxtran and ferucarbotran. Experimental studies show that MNP-enhanced MRI is vastly superior to other noninvasive methods of identifying lymph node metastases from solid tumors and histologically positive lymph nodes outside of the usual field of resection. MNP application in delineating primary tumors and detecting metastases, in imaging angiogenesis and mapping vascular supply to primary tumors has a realistic translational potential. Macrophage-specific MNP labeling protocols are used to image inflammatory pathologies, including atherosclerosis, multiple sclerosis and rheumatoid arthritis. Long-term MRI-guided in vivo cell tracking of CNS regeneration became possible with the use of grafted MNP-labeled stem cells and neuroprotective glia (Schwann cells and olfactory
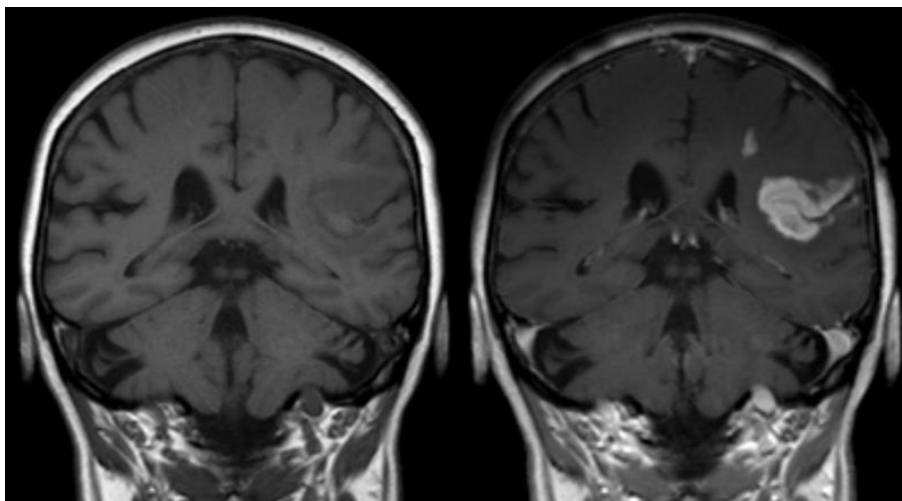

Figure 15: MRI image before and after the injection of MNPs

ensheathing cells). FITC-conjugated MNPs have been used by surgeons to delineate gliomas both preoperatively, based on their MRI modality, and intraoperatively, based on fluorescent tag. This is particularly valuable since certain tumors, such as gliomas, can shift position during surgery [18].

MRI has advanced to cellular and molecular sensitivities, with nanofunctionalized MRI contrast agent libraries now available. For example, the HIV-derived TAT peptide conjugated to ultrasmall iron oxide MNP allows efficient T cell labeling within 5 minutes. A number of studies demonstrate the immense potential of MNP-based molecular MRI as a combination imaging and drug/gene delivery strategy. For example, monocrystalline iron oxide MNPs (3 nm core) sterically protected by a layer of low-molecular weight dextran and covalently conjugated to holo-transferrin, promotes overexpression of engineered transferrin receptor (ETR) to selectively visualize tumors in vivo in real time at exceptionally high spatial resolution [18].

5.5 Bioseparation and biosensors

In vitro streptavidin-coated magnetic beads are used for phenotypic selection in different cell sorting protocols, including stem cells, sensory neurons and others. Conjugated to monoclonal antibodies, MNPs could be used to decontaminate blood from infective agents. The principles of MNP-based magnetic bioseparation have been applied to integrative biosensor technologies. For example, ultrasensitive bio-barcodes can detect protein analytes using specific MNP-conjugated antibodies, followed by dehybridization of the co-tagged oligonucleotides [18].

5.6 Targeted drug delivery

The development of drug delivery systems with selectivity to pathologic sites is an ambitious goal. The principles of magnetic guidance of MNP-conjugated drugs have been applied experimentally, and have reached clinical trials as a cancer therapy. Following i.v. delivery of MNPs, an external magnetic field is used to concentrate MNPs at a specific target site; this procedure has been well tolerated in cancer patients. Nanoparticle-based drug and gene delivery systems may solve the insurmountable obstacle of treating neurological diseases: delivery across the blood–brain barrier. But issues of potential embolization with MNP aggregates in capillaries and the necessity for large distances between the pathological site and external magnetic field still present a challenge. When

considering the MNP surface chemistry for drug delivery, it is favored that MNPs retain sufficient hydrophilicity and, with coating, do not exceed 100 nm in size to avoid rapid clearance by RES. Overall, the smaller, more neutral and more hydrophilic the nanoparticle surface, the longer its plasma half-life [18].
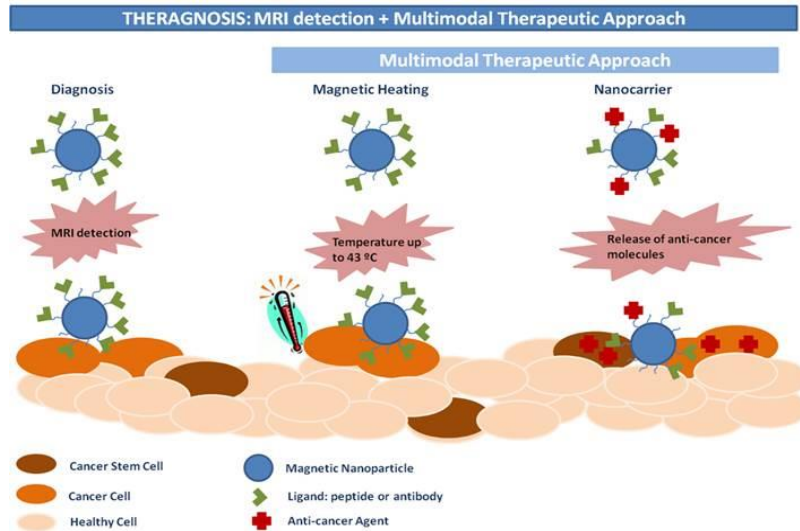

Figure 17: Drug delivery

5.7 Magnetic transfections

When functionalized with DNA vectors, MNPs could be used as effective gene transfection systems under external magnetic field, termed magnetofections (MF). Direct comparison of state-of-theart magnetic polycation polyethylenimine-coated MNP and corresponding standard gene vectors demonstrated a profound increase in transfection efficiency for both nonviral and viral vectors in permissive and non-permissive cells. In endothelial cells, MF increased the efficiency of the luciferase reporter by 360-fold and effective antisense oligonucleotide delivery in vivo and in vitro. An example of magnetic nonviral gene transfer protocol includes steps of MNP synthesis, testing intact DNA binding with MNP core, preparation of magnetic lipoplexes and polyplexes, magnetofection and data processing [18].
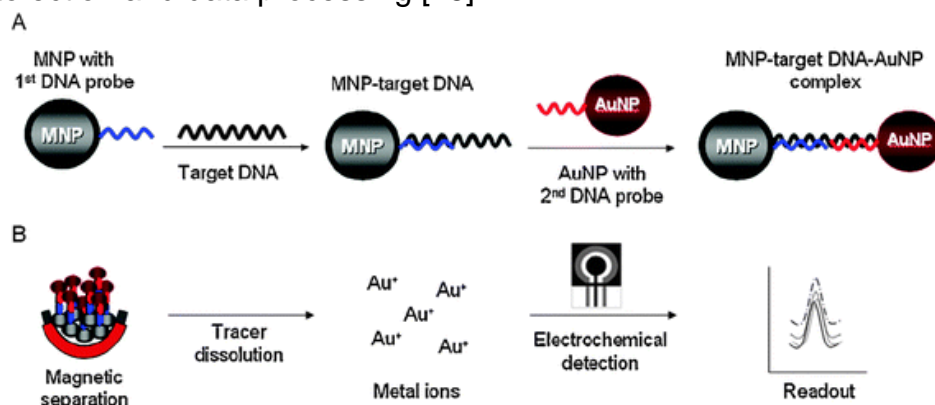

Figure 18: Transfection process

5.8 Tissue engi neering

Iron oxide MNPs have several distinct applications in tissue engineering. They have been used in stem cell replacement therapy for cell labeling, sorting, monitoring, engraftment and targeted in vivo delivery. MNPs can be also used to weld the joining tissue surfaces under high temperatures, a process typically accompanied by protein denaturation followed by re-polymerization of adjacent protein chains. With regard to nanomagnetic welding, gold and silica coating are expected to increase MNP sensitivity and robustness to light absorption and allow for selection of light sources and wavelengths with minimal damage to tissues. Magnetic nanoparticles have been used for construction and harvesting of multilayered keratinocyte sheet-like 3-D constructs. Self-assembled magnetic nanowire arrays could potentially be used in tissue engineering [18].

5.9 Iron detection and chelation therapy

Excess metal deposits are associated with virtually every neurodegenerative disease, including multiple sclerosis, Friedreich's ataxia, Alzheimer's, Parkinson's, and Huntington's diseases. Advanced technologies of nano-sized iron detection in neuronal tissues, such as by superconducting quantum interference device (SQUID) magnetometry, have found use as a diagnostic strategy in identifying iron deposits in the brains of Alzheimer's and neuroferritinopathy patients. As experimental therapeutics, MNPs may be used as iron chelators for neurodegenerative diseases, potentially presenting another theragnostic application [18].

5.10 Magnetic immunoassay

Magnetic immunoassay (MIA) is a novel type of diagnostic immunoassay utilizing magnetic nanobeads as labels in lieu of conventional, enzymes, radioisotopes or fluorescent moieties. This assay involves the specific binding of an antibody to its antigen, where a magnetic label is conjugated to one element of the pair. The presence of magnetic nanobeads is then detected by a magnetic reader (magnetometer) which measures the magnetic field change induced by the beads. The signal measured by the magnetometer is proportional to the analyte (virus, bacteria, cardiac marker, etc,) quantity in the initial sample [2].

5.11 Supported enzymes and peptides

Enzymes, proteins, and other biologically and chemically active substances have been immobilized on magnetic nanoparticles. They are of interest as possible supports for solid phase synthesis.

This technology is potentially relevant to cellular labelling/cell separation, detoxification of biological fluids, tissue repair, drug delivery, magnetic resonance imaging, hyperthermia and magnetofection [2].

5.12 Genetic engineering

Magnetic nanoparticles can be used for a variety of genetics applications. One application is the rapid isolation of mRNA. In one application, the magnetic bead is attached to a poly T tail. When mixed with mRNA, the poly A tail of the mRNA will attach to the bead's poly T tail and the isolation takes place simply by placing a magnet on the side of the tube and pouring out the liquid. Magnetic beads have also been used in plasmid assembly. Rapid genetic circuit construction has been achieved by the sequential addition of genes onto a growing genetic chain, using nanobeads as an anchor. This method has been shown to be much faster than previous methods, taking less than an hour to create functional multi-gene constructs in vitro [2].

6 MNP biodistribution, clearance and toxicity

6.1 MNP metabolism

Typically, upon their intracellular internalization via endocytosis, MNPs are clustered within lysosomes where, presumably, they are degraded into iron ions by an array of hydrolyzing enzymes at low pH according to endogenous iron metabolism pathways. MNP size, charge, surface chemistry and route of delivery each influence their circulation time and biodistribution patterns in the body. Large (>200 nm) particles are usually sequestered by the spleen via mechanical filtration followed by phagocytosis, whereas smaller <10 nm particles are rapidly removed through extravasation and renal clearance, with particles 10–100 nmbelieved to be optimal for i.v. administration. The typical final biodistribution of particles is 80–90% in liver, 5–8% in spleen and 1–2% in bone marrow [5]. Surface chemistry dictates the efficiency and the mechanism of MNP internalization by cells as well as their overall biodistribution in organ systems, metabolism and potential toxicity. Depending on the routes of their

delivery/exposure, MNPsurfacesmay interact with extracellular matrix components and the plasma cell membranes of macrophages, endothelial cells, skin epithelium, and respiratory or gastrointestinal tracts. A point worth noting is that MNPs accumulate in the brain, liver, spleen and lungs after their inhalation, demonstrating their ability to cross the blood–brainbarrier. MNPs can also penetrate the hair follicles and stratum corneum, reaching viable skin epidermis [18].

6.2 Macrophages in nanoparticle clearance: a double-edged sword

Upon their in vivo administration, within minutes nano-sized particles are challenged by macrophages of the RES. The efficacy of particle clearance by the RES depends upon the size, chemical composition, cumulative projected area and surface chemistry of the MNPs and can influence mechanisms of macrophage activation and particle internalization.

Multiple mechanisms of intracellular internalization of nanoparticles have been described, including phagocytosis (mediated by mannose, complement, Fcγ and scavenger receptors) and endocytosis (clatrin- and calveolin-mediated, fluid-phase). MNPs have been reported to be internalized via phagocytosis, scavenger receptormediated endocytosis, fluid-phase endocytosis and diffusion. Depending on surface hydrophobicity and charge, nanoparticles can get opsonized by plasma proteins (e.g., albumin, apolipoprotein, immunoglobulins, complement, fibrinogen), which promotes their recognition and clearance by cells of RES. Opsonization can change the mechanisms of particle uptake by cells of RES. For example, iron oxide MNP binding to plasma fibronectin and vitronectin changed from receptor-mediated to fluid-phase endocytosis. Efforts are made to engineer MNPs of size and surface chemistry that will minimize their opsonization and macrophage-mediated clearance and thus increase their circulation time. For example, surface coating with amphiphilic polymeric surfactants, such as polyethylene glycol (PEG), significantly reduces MNP interactions with plasma proteins, minimizing their internalization and clearance by macrophages. But because PEG-coated MNP uptake is highly efficient, it is anticipated that their cytotoxic potential in nonimmune cells will be increased. It is likely that cytotoxic dedifferentiation and cell death after exposure to anionic DMSA-coated MNPs (AMNPs) relates to the very efficiency of uptake, resulting in dose-dependent intracellular iron overload. In vitro, AMNPs are internalized by macrophages and neuron-like PC12 cells and other cells. In fact, their rapid and efficient

internalization was noted to be uniform between 14 different cell types in vitro, including hepatocytes, fibroblasts, smooth muscle cells, stem and progenitor cells and immune cells. MNPs internalization by macrophages is mediated via integrin MAC-1 (also known as CD11b, CD18) and scavenger receptors SR-A.

It is not yet clear whether in vivo AMNPs are internalized uniformly between the cells, particularly immune or non-immune tissue cells. Potency of macrophages to "sense", migrate towards and phagocytose nanoparticles depends highly on MNP surface chemistry, and occurs typically 6–12 h after their in vivo exposure. In addition, inherent immunocompetence of organ and tissue systems is likely to play an important role. For example, immunocompetence of the nervous system is not homogenous. Peripheral nerve is capable of recruiting highly potent macrophages that, by clearing degenerating debris, creates a permissive environment for neurite growth. This immunocompetence is believed to promote the propensity of peripheral nerve for regeneration, in great contrast to the central nervous system (CNS), where macrophages are few and ineffective. We found AMNPs to stimulate macrophage recruitment into peripheral nerve 24 h after their injection, where they seem to predominantly label infiltrating macrophages. Thus, MNP microinjection into peripheral nerve may present an advantageous experimental model for studying the MNP–macrophage interface within a mammalian nervous system, preventing MNP clearance issues characteristic of intravenous delivery. Understanding the molecular interactions at the macrophage–nanoparticle interface has led to new approaches for selective MR imaging of cardiovascular diseases, multiple sclerosis, stroke and other diseases.

Macrophages are critical elements in the body's defense system against diseases, and introduction of nanoparticles into the body may affect macrophage defensive function. It is known that nanoparticles promote activation as well as phagocytotic, cytoskeletal and cytokinereleasing functions of macrophages. Dextran-coated MNPs induce differentiation of monocytes into macrophages. While proinflammatory signaling may manifest macrophage activation, it may mediate MNP-induced macrophage cytotoxicity. Given that particle clearance by macrophages is size-dependent, ultrasmall nanoparticles can escape phagocytosis and lavage within the macrophages, promoting activation of oxidative stress and ROS-mediated redoxsensitive transcription via NF-κB and AP-1, proinflammatory TNF-α/p38 signaling and apoptosis. In fact, these

properties have translated into therapeutic «macrophage-suicide» approaches of nanocarrier systems for macrophage-driven diseases of bacterial infection, atherosclerosis, rheumatoid arthritis and neuroinflammation. However, the limited selectivity of such designs to macrophages due to often similar cell surface composition in other immunocompetent cells, such as Schwann cells and microglia in the nervous system, as well as the adverse effects of macrophage destruction on local and central immunity, should be considered in the overall scheme of nanotoxicity. Inhibition of p38 MAPK by SB- 239063 reduces uptake of MNPs by aortic macrophages after their i.v. administration, providing a potential strategy to modulate MNP toxicity in vivo.

Based on the multi-factorial relationship of MNPs with macrophages, engineering strategies to increase the ability of MNPs to evade macrophages have to be accompanied by thorough evaluation of their toxic potential associated with relevant routes of delivery and identification of target cells of their internalization. Intrinsic to their enhanced reactive surface area, propensity to cross tissue and cell barriers, and ability to lavage within cells, nano-sized materials can compromise functions of cell membranes, mitochondria, nuclear membranes and DNA [18].

6.3 Oxidative stress: a paradigm for nanotoxicity

Iron oxide MNPs are believed to induce redox cycling and catalytic chemistry via the Fenton reaction [$H_2O_2+Fe^{2+}\rightarrow Fe^{3+}+HO^-+HO^*$], the most prevalent source of reactive oxygen species (ROS) in biological systems. In fact, uncoated magnetite nanoparticles are significantly cytotoxic. But the mechanism of cytotoxicity of the fully oxidized (Fe_2O_3) maghemite MNPs is not directly explained by the Fenton chemistry. Furthermore, ROS generation leading to oxidative stress (OS) is associated with the nanotoxicity of nonmetal nanoparticles as well. While the mechanisms by which nanoparticles generate ROS are still largely unknown, it is hypothesized that disruption of the well-structured electronic configuration of the nano-sized material surface creates reactive electron donor or acceptor sites, leading to the formation of superoxide radicals. As a multistage process, nanoparticle-induced ROS activation induces defense antioxidant response elements by the transcription factor Nrf-2, leading to increased expression of over 200 phase II antioxidant enzymes, such as heme oxygenase 1 (HO-1) and superoxide dismutase (tier I OS). If damage proceeds, protective systems are superseded by mitogen-activated protein kinase (MAPK)

and NF-κB-activated intracellular signaling, resulting in proinflammatory cytokine, chemokine and matrix metalloproteinase (MMP) release (tier II OS), leading to apoptosis (tier III OS). Current studies on mechanisms of nanotoxicity overwhelmingly point to OS mediated activation of proinflammatory cytokines and MAPK signaling pathways in respiratory and gastrointestinal tracts, blood cells, skin and the nervous system, as carefully reviewed. A continuum of molecular events from tier I to III OS manifested through increased HO-1 and JNK-mediated TNF-α production leading to apoptosis. Studies into the effects of NP size, shape and state of dispersion indicate a clear correlation between these physiochemical characteristics with cytotoxicity and the cellular proinflammatory response.

Tier II OS can manifest in vivo through immune cell infiltration, mediated by the actions of proinflammatory cytokines and MMPs. For example, ROS controls MMP activity by two distinct mechanisms: MAPK-induced overexpression of MMP gene and directly through structural oxidative modification of thiol residues on inactive pro-MMPs, resulting in release of the zinc-binding domain and MMP activation. In Fig. 3 we summarize our hypothesis of ROS-induced MMP activity in the nervous system leading to increased blood–brain-barrier (BBB) permeability and neuronal damage. In support of this hypothesis, MMPs are proposed to mediate (and present a highly sensitive measure for) macrophage activation in response to nanoparticles. Internalization of chitosan-coated MNPs promotes invasive potential of cells into the 3-D-porous scaffolds via MMP action. MNPs are believed to promote cytotoxicity of human fibroblasts through the action of proinflammatory cytokines and MMPs, which are considered to be useful biomarkers for metal toxicity. In the context of AMNPinduced macrophage recruitment into the nerve it is worth noting that cytokines and MMPs are important modulators of macrophage recruitment into the nerve Together, these studies support a model in which MNPs induce ROS to promote MMP-mediated degradation of the blood–brain and blood–nerve barriers to promote recruitment of macrophages into the nervous system.

6.4 Metals and MNPs in neurodegeneration

While iron oxide is considered safe, imbalance in its homeostasis has known toxic implications to many organ systems. As th abundant, redox-active metal, iron facilitates the generation of free radicals in the brain and excess iron is associated with multiple neurodegenerative disorders, including multiple sclerosis, Alzheimer's and Parkinson's diseases. We have mentioned that nano-

scale iron oxide deposits have been identified in neurological tissues using SQUID magnetometry in the brains of Alzheimer's patients and basal ganglia of neuroferritinopathy patients. These iron nanoparticles are believed to be biogenic in nature and linked to ferritin, a large (12 nm) natural ferric oxide phosphate storage protein. However, evidence of brain accumulation of MNPs after passive exposure through inhalation calls for confirmation of the source of MNP deposits in the brains of neurodegeneration patients. It is particularly important due to the ability of MNPs to penetrate through skin and cross blood–brain barrier after exposure through inhalation and by intraperitoneal delivery. Studies on the neurotoxicity of MNPs and identifying their safe formulations are required prior to their therapeutic use as an iron chelating therapy for neurodegenerative disorders and drug conjugates (e.g., glial derived neurotrophic factor) as a therapy for drug addiction.

6.5 Current studies of MNP toxicity

Given the variety of MNP formulations and their biomedical applications, the limited number of studies evaluating their toxicity is astounding. The findings on iron oxide range from cytotoxicity in vitro to transient and acute in vivo toxicity to unremarkable changes in vivo. In relevance to the journal's Theme Issue of nanoparticle toxicity, in this section we refer to toxic properties of iron oxide and other metal and metal oxide MNPs.

MNP cytotoxicity to non-immunogenic cells in vitro is increasingly being noted, in addition to that in macrophages reviewed above. Several metal oxide nanoparticles of 20–45 nm produced dose-dependent apoptosis and membrane function in mouse neuro-2A cells that were measured by membrane leakage of lactate dehydrogenase and MTT reduction. In studying the capacity of AMNPs to extend neurite outgrowth under magnetic force, we observed dedifferentiation and cell death of neuron-like PC12 cells with increasing concentration of iron oxide. Although DMSA itself (used for coating) did not cause toxicity and is a known non-toxic BBB-crossing therapeutic chelator of metal, it presents an efficient cellular internalization system of iron-oxide MNPs, resulting in intracellular overload with iron. Because target intracellular compartments of iron oxide MNPs include mitochondria and nucleus, increase in oxidative stress-related changes and gene expression can occur. In fact, MNPs of various compositions, sizes and even at mild exposures can activate proinflammatory and ROS-induced cell signaling, as well as interference with mitochondrial energy

production in cultured cells. However, of several MNPs comparatively tested, iron oxide MNPs were shown to be the safest, producing cytotoxic changes at levels of 100 μg/ml or higher. Reduced cytotoxicity of oxide nanoparticles is associated with increased particle solubility and modification of surface chemistry.

In vivo toxicity data on MNPs is hopeful, demonstrating no longterm implications of their use when administered at clinically relevant concentrations via relevant routes. Several reports found iron to accumulate in tissues, but with unremarkable histological changes in vital organs, concluding safety of the respective formulations. Although MNP deposits were detectable in the prostates of prostate cancer patients after a year of magnetic hyperthermia therapy, no signs of systemic toxicity were found. The median lethal dose (LD_{50}) of dextran-coated magnetite MNPs is very high at 400 mg/kg in rats, with cytotoxic effects on peritoneal cells, lymphocytes and neutrophils. Hemangiectasia and leukocyte infiltration observed after single subcutaneous administration of dextran-coated MNPs almost disappeared 72 h after their administration. Signs of oxidative stress, evident in spleen and to a lesser degree kidney and liver of rats after intravenous administration of oleic acid-pluronic-coated iron oxide MNPs, gradually declined after 3 days of administration. As mentioned, MNP surface chemistry that ensures high efficiency of intracellular MNP uptake or effective evasion of the RES is likely to increase their toxic potential.

Although the studies on MNP toxicity are limited in number, they point at the influence of MNP composition, size, dispersibility, surface chemistry and the regimens of their administration in the toxic outcomes as anticipated. Next, we will outline the influences of testing and study design on nanotoxicity data.

6.6 Intricacies of nanotoxicity testing and data analyses

The necessity, purpose and directions in the formation of the new discipline of nanotoxicology have been discussed in detail, and MNPs bear no exception. Physiochemical characteristics of nanoparticles (size, shape, surface chemistry, solubility) each influence their toxic potential. Particokinetics and dosimetry approaches to nanotoxicity assessment encompass measures for dose of exposure (mass administered, media mass, surface area), delivered dose (number per cell or cm^3), and cellular dose (internalized mass). With many parameters to assess, the demand for toxicity evaluation exceeds current capabilities of the research field. Thus, prioritization of the physicochemical

parameters of clinical relevance to the target organ groups is imperative. E.g., for skin, that includes NP dissolution, size and partition coefficient, whereas for brain, hydrophobicity and surface chemistry, relating to possibility to cross barriers, size and shape and chemical composition are more relevant.

It has been suggested that study designs center only on clinically relevant target cells and include in-depth mechanistic analyses of the hierarchical process of oxidative stress (OS). For tier I OS, ROS species generation and measures of anti-oxidative HO-1 have been proposed as useful measures of OS-specific nanotoxicity. As mentioned already, activation of proinflammatory signaling and MMPs have been adopted by many studies and represent reliable measures of tier II OS. It has been shown, however, that measures of MMP-9 provide higher sensitivity when cytokine measures fail. Overall, the use of multiple assays is important to avoid false-positive or false-negative results. Tier III OS can be identified by activation of pro-apoptotic pathways. Thus, whether or not activation of tier I OS would indicate ROS-induced changes of nanotoxicity, determination of cell apoptosis of tier III OS will help understand the extent of cytotoxicity. In vivo, the cell source for specific changes could be identified by dual-labeling of OS-specific antigens and cell specific markers using confocal microscopy. Caution in the interpretation of mechanistic studies is important and a consideration that low-level ROS signaling contributes to normal cellular redox signaling and cytokine-protease activation may relate to the body's defense reaction in immobilizing immune cells.

For in vivo nanotoxicity assessment, cell viability and mechanistic OS measures should be supplemented by evaluation of organ-specific toxicity, such as renal filtration or blood–brain barrier breakdown. The biokinetics of nanoparticles through confirmed and potential routes of exposure involves multiple pathways of their translocation prior to clearance, particularly as nanoparticle binding to proteins generates complexes that are more mobile and pervasive through tissues normally inaccessible. The time-course of nanotoxicity measures may help reconcile studies demonstrating safety of MNPs with those of transient and acute in vivo toxicity. Direct comparison of in vivo and in vitro pulmonary nanotoxicity using the same assays showed little correlation, as NP biodistribution and RES clearance both factor in their in vivo toxicity. Toxicity of MNPs in normal and pathologic tissues may also differ due to the differences in

their cell composition and phenotypic status (e.g., availability of specific receptors to mediate MNP endocytosis), and should be addressed independently.

Some toxicity data may not be specific to nanoparticles per se, but relate to the increased substance quantities and accumulation, which could be adjusted with adoption of appropriate concentration standards. Since most substances become toxic at high doses, it is important that nanotoxicity studies incorporate doses at the anticipated human exposures. Toxicity could also be qualitatively different based on size, surface chemistry or specific interaction. When nanotoxicity is observed, the role of each component of the composite structure should be evaluated as control factors, if possible (e.g., its vehicle or coating material). For example, polyakylcyaniacrylate- coated MNPs (220 nm, with 10–20 nm cores) showed an LD_{50} of 245 mg/kg, however, a similar LD_{50} was observed in polyakylcyaniacrylate (not MNP-based) particles.

7   Experimental process

The first step in the synthesis of the magnetic nanoparticles is to prepare a solution of NaOH having a concentration 1.5M(15g) dissolved in 250 ml of distilled water. By other side, another solution was prepared, in this case 100 ml of 10mM of HCl in 100 ml of distilled water.
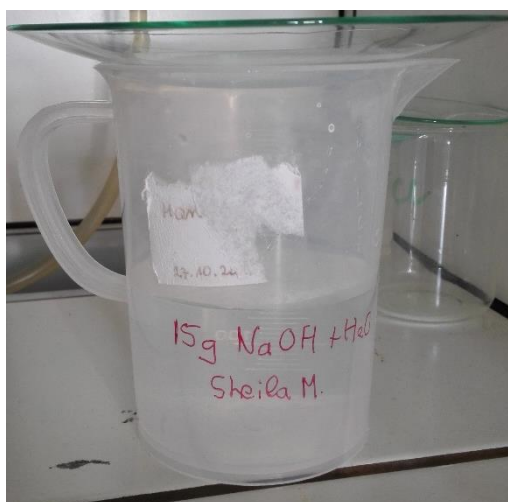
*Figure 18: Solution of NaOH+H_2O*
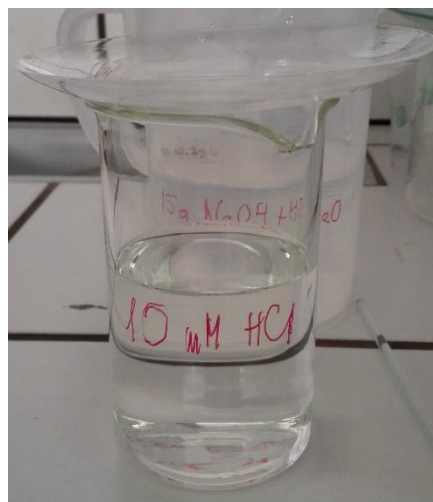
Figure 19: Solution of HCl+H_2O

The next step was to weight the necessary amount of Iron Chlorides (FeCl$_3$·6H$_2$O and FeCl$_2$·4H$_2$O) for its later dissolution in 25 ml of the HCl+H$_2$O solution (Figures 20 and 21). Immediately, the NaOH+H$_2$O solution was heated until 80ºC, once the temperature has been reached the solution of iron chlorides in HCl was added slowly (Figure 22). For this step is necessary to use a moderate mixing and a condenser to avoid the evaporation.
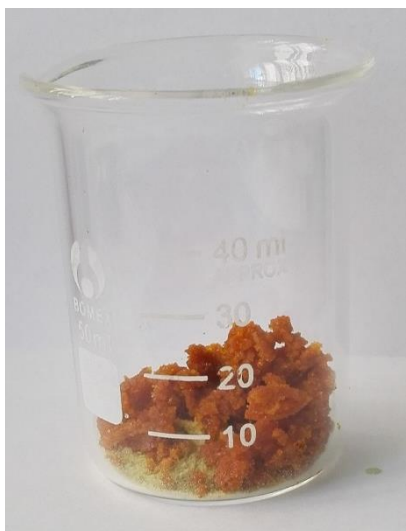

Figure 20: Iron chlorides.

Figure 21: Solution of iron chlorides in aqueous solution of HCl.
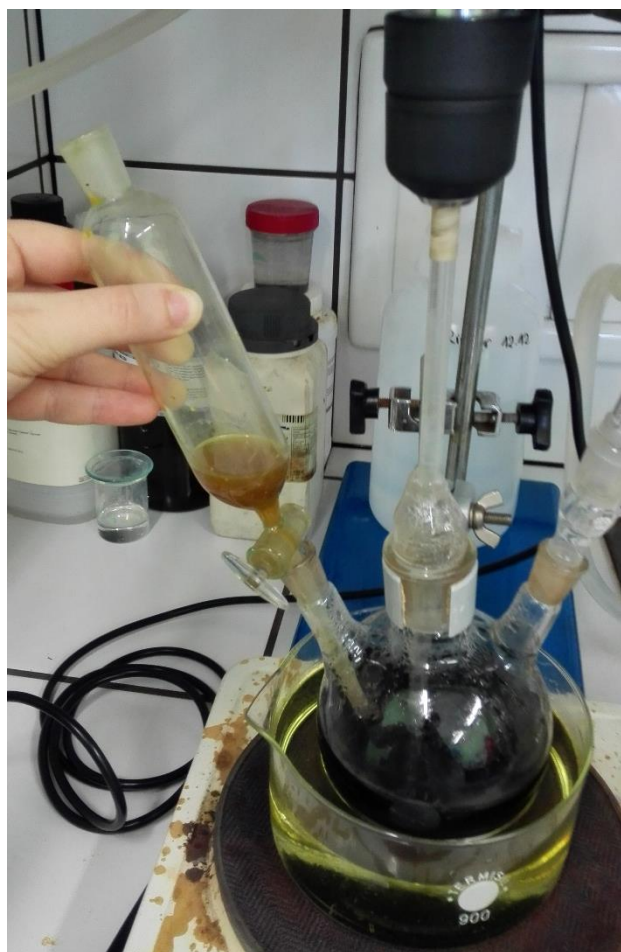
Figure 22: Dropping of acidic solution of iron chlorides into the NaOH solution.

Once the solution has been added and is completely mixed is necessary to let it cool down. The dark color of the solution is an indicator of the presence of the magnetic nanoparticles. During the cooling down process was possible to see how the nanoparticles and the agglomerations precipitate to the bottom of the 3-neck distillation flask (Figure 23). A continuation, the solution is poured down to the beaker and submitted to a magnetic field crated by a magnetic stirrer which affects the magnetic nanoparticles and make the precipitate to the bottom of the

beaker (Figure 24). After 15-20 minutes applying the magnetic field the excess of solution is removed and 140 ml of distillated water is added to clean the nanoparticles. The magnetic field is applied again for a new precipitation of the magnetic nanoparticles and again the excess of solution is removed carefully. This procedure can be carried out as many times as deemed necessary. After cleaning the nanoparticles is necessary to store them into a closed recipient in a cooled temperature.
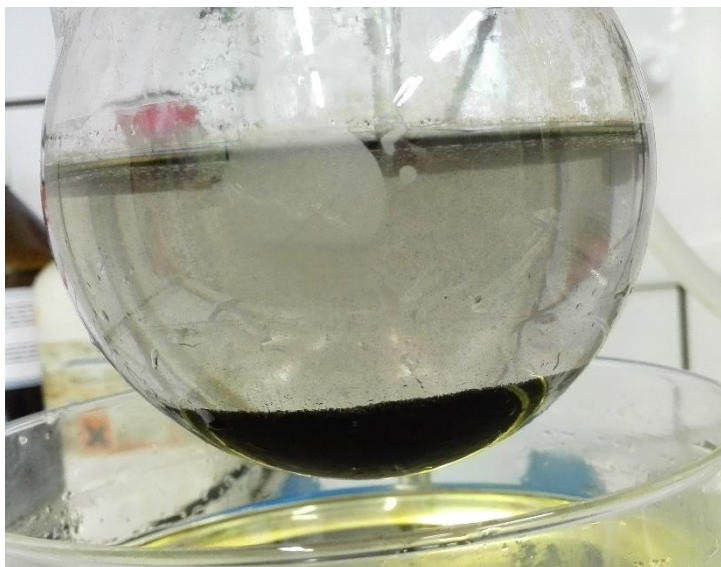
Figure 23: Precipitation of the magnetic nanoparticles.
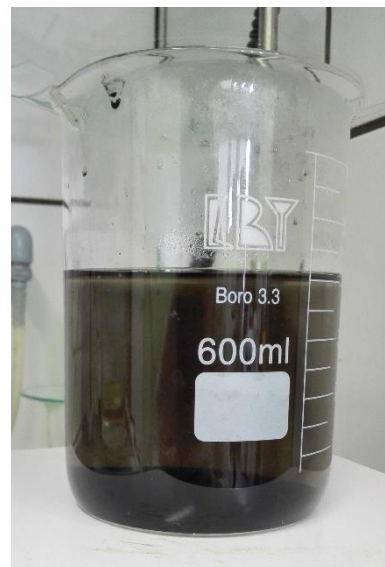
Figure 24: Precipitation of the magnetic nanoparticles due to the magnetic field.

The following step is the preparation of 3 solutions whose function is stabilize and avoid the agglomeration of the nanoparticles. First 2 solutions of 140 ml of distillated water with a concentration of 3% Gum Arabic will be prepared. The 3d one will be 140 ml of lavender essential oil and also a concentration of 3% Gum Arabic. Once the solutions are prepared the procedure is the same for the three of them.

The procedure for the synthesis on the magnetic nanoparticles consist in heating the solution of Gum Arabic with 7.5 ml of magnetic nanoparticles solution until 80ºC, heat it for 2 hours at that temperature, after add 3.75 ml of $HAuCl_4 \cdot 4H_2O$ and 1.5 ml of $NH_2OH \cdot HCl$, finally mix such prepared mixture for next 15 minutes and let it get cold. The conditions for this procedure were as follows: continuously mixing, controlled temperature and a condenser with continuously flow of cold water and an inert atmosphere with Argon gas. For the first solution apart from the Gum Arabic solution and the magnetic nanoparticles 100 ml of distilled water were also added at the beginning of the heating process.

For the second solution apart from the Gum Arabic solution and the magnetic nanoparticles 100 ml of lavender essential oil were introduced, also at the beginning of the heating process. In the case of the third solution reaction mixture consisted only in 3% solution of Gum Arabic in solution containing lavender essential oils. In the following Figure 25 the equipment used for the synthesis is shown.

To prevent the degradation and agglomeration, $HAuCl_4 \cdot 4H_2O$ and hydroxylamine were added into previously prepared mixture after heating for 2 hours at 80ºC to obtain nanogold particles that will form a layer on the magnetic nanoparticles surface.
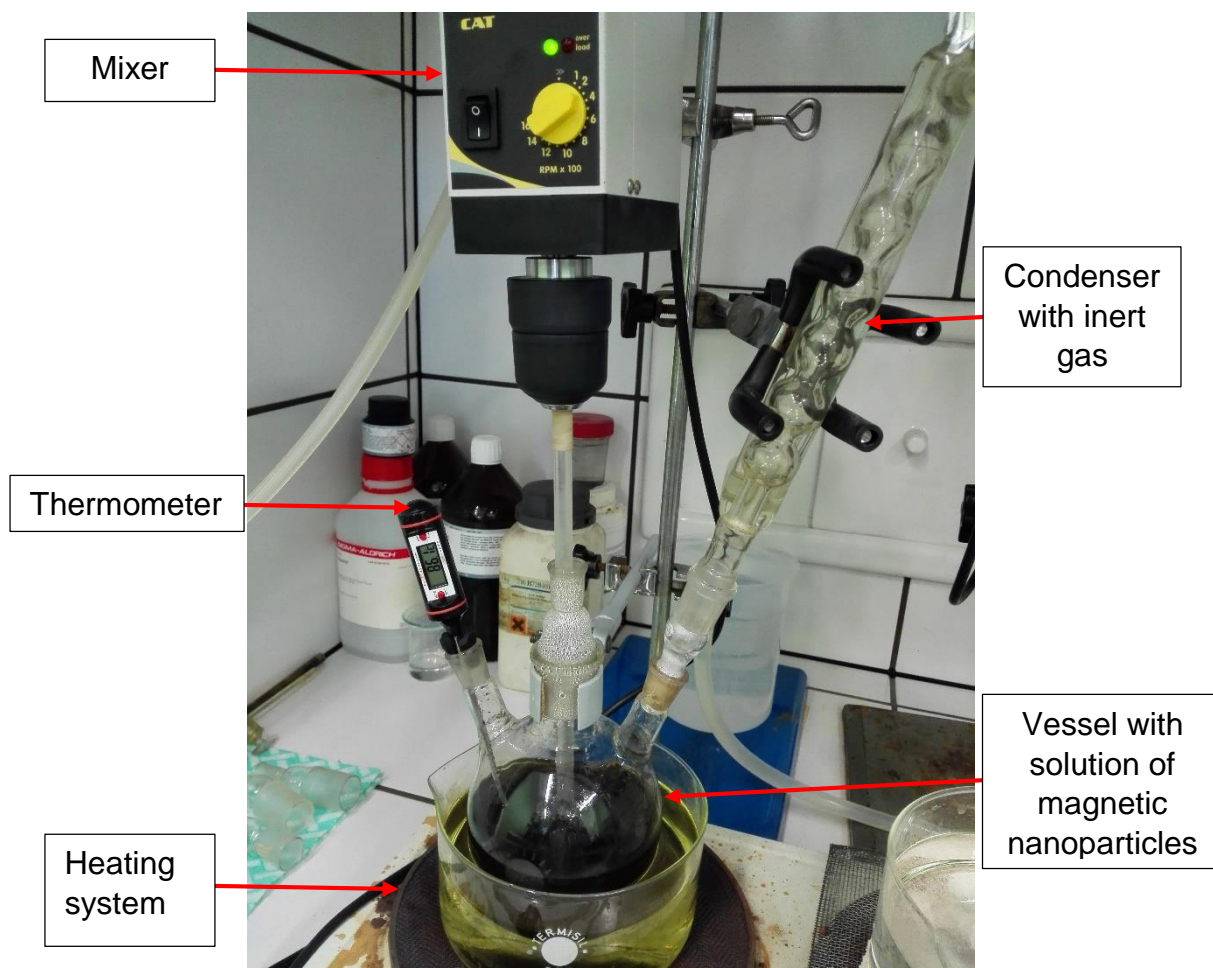

Figure 25: Synthesis equipment.

8 Results

After the synthesis of magnetic nanoparticles, analysis of their size and distribution ware performed by using Dynamic light scattering (DLS) technique. DLS is a technique in physics that can be used to determine the size distribution profile of small particles in suspension or polymers in solution. As in the introduction of this report has been said the size of the particles has to be between 1-100 nanometers in diameter to consider them nanoparticles.

The first DLS result was obtained for nanoparticles after Massart synthesis (only iron chlorides in alkaline solution) that is the common step in all the procedures (Graph 1).
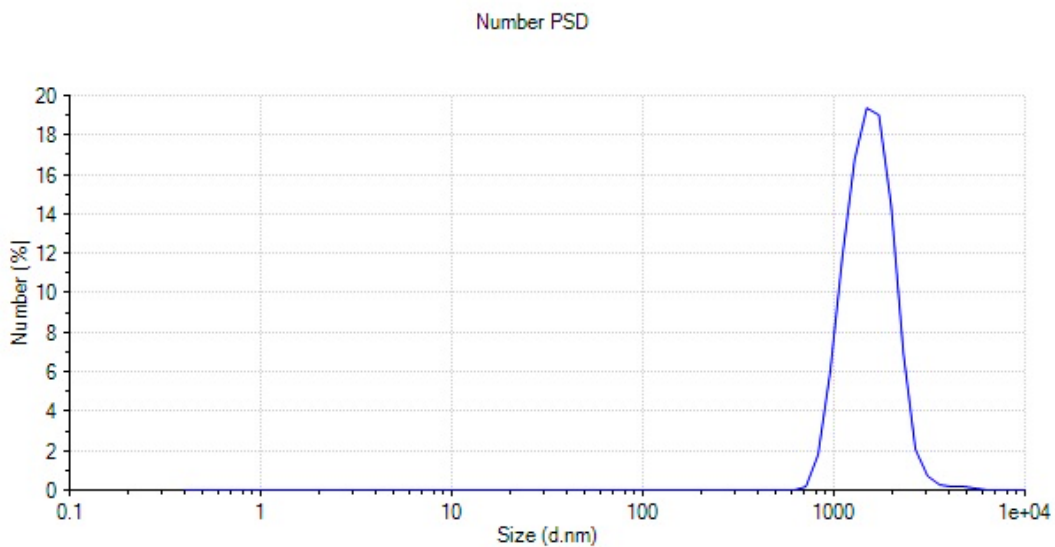
Graph 1: Size of particles after Massart synthesis

The average size of the particles is 2720 nm. This indicates that there aren't nanoparticles but bigger particles or/and nanoparticles agglomerations can be found in obtained mixture.

The second DLS result derived from nanoparticles after Massart synthesis and stabilized with Gum Arabic solution plus additional 100 ml of distilled water (Graph 2)
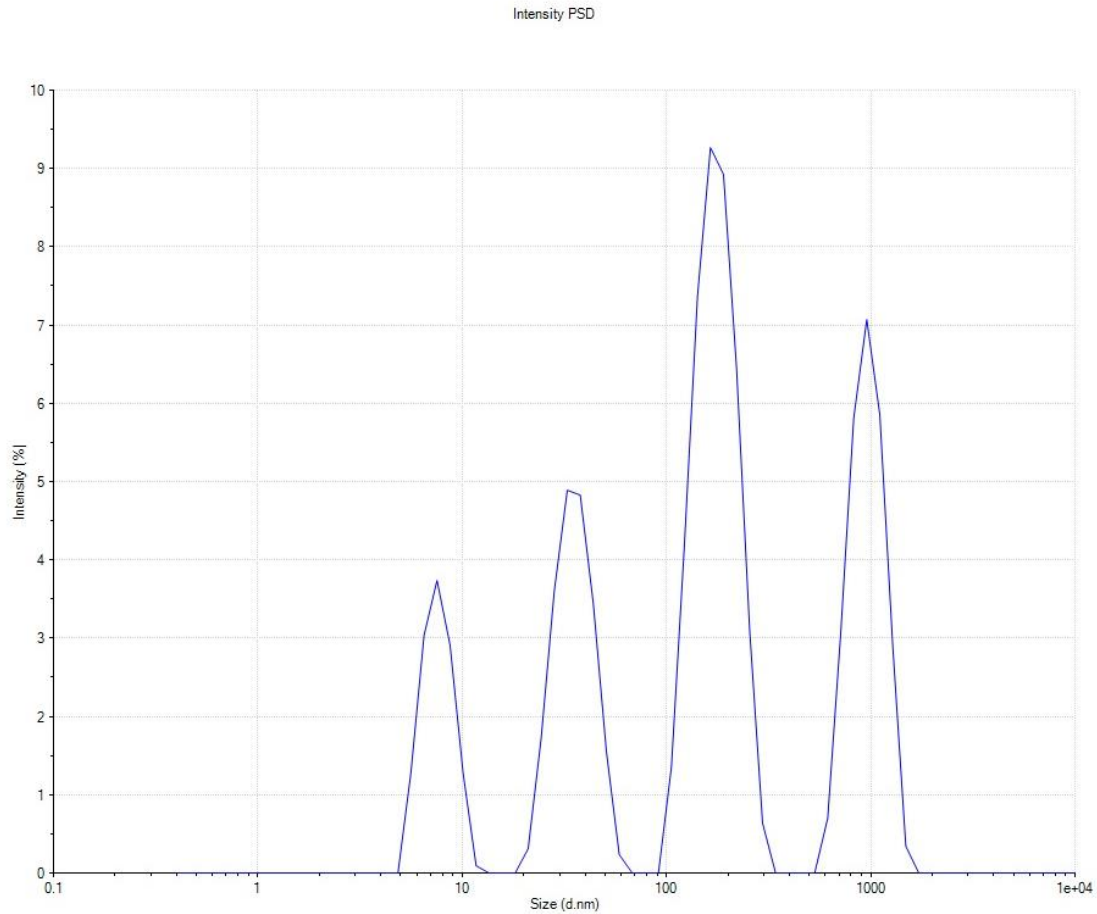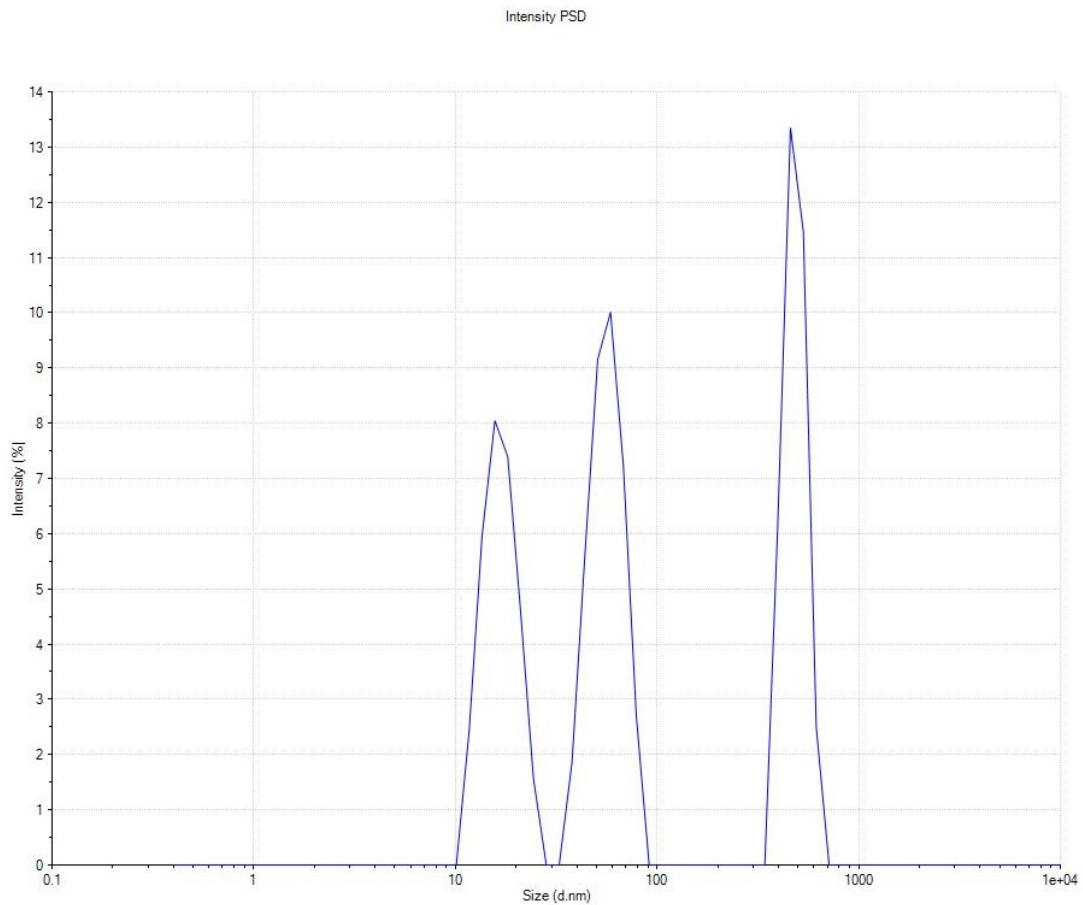

Graph 2: Size of particles after the stabilization with solution of Gum Arabic and distillated water.

Based on the graph shown below it can be stated that the average size of obtained particles is 422 nm. In the Graph 2 a big polydispersity of the particles size can be observed, but there are nanoparticles which sizes are less than 100 nm, even less than 10 nm. Therefore, it is assumed that the addition of the stabilizing agent has a huge impact on the obtainment of nanoparticles.

The third DLS result derived from nanoparticles after Massart and second step in which nanoparticles have been introduced into Gum Arabic solution plus additional 100 ml of lavender essential oil (Graphs 3 and 4)
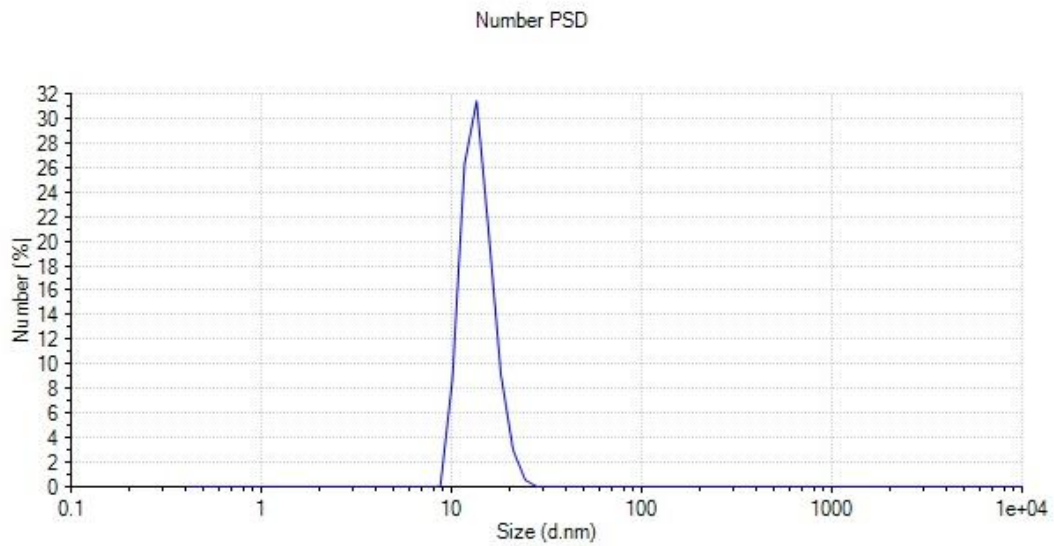
Graph 3: Size of particles after the stabilization with solution of Gum Arabic and lavender essential oil (Number).

Graph 4: Size of particles after the stabilization with solution of Gum Arabic and lavender essential oil (Intensity).

As can be seen in Graph 3 there are only nanoparticles, above the 31% of the particles have a size about 15 nm. One important information: as it can be seen result have been given in two ways: including intensity and number.

Number is the most important because it most accurately shows what types of particles the solutions have.

In case of intensity, results could be misleading because bigger particle scatters most of the light and "covers" nanoparticles. Therefore, it is significantly better to determine sizes looking at "number" graphs.

Finally, the fourth DLS result derived from nanoparticles after Massart and stabilization in the following conditions: solution of Gum Arabic in lavender essential oil (Graphs 5 and 6).
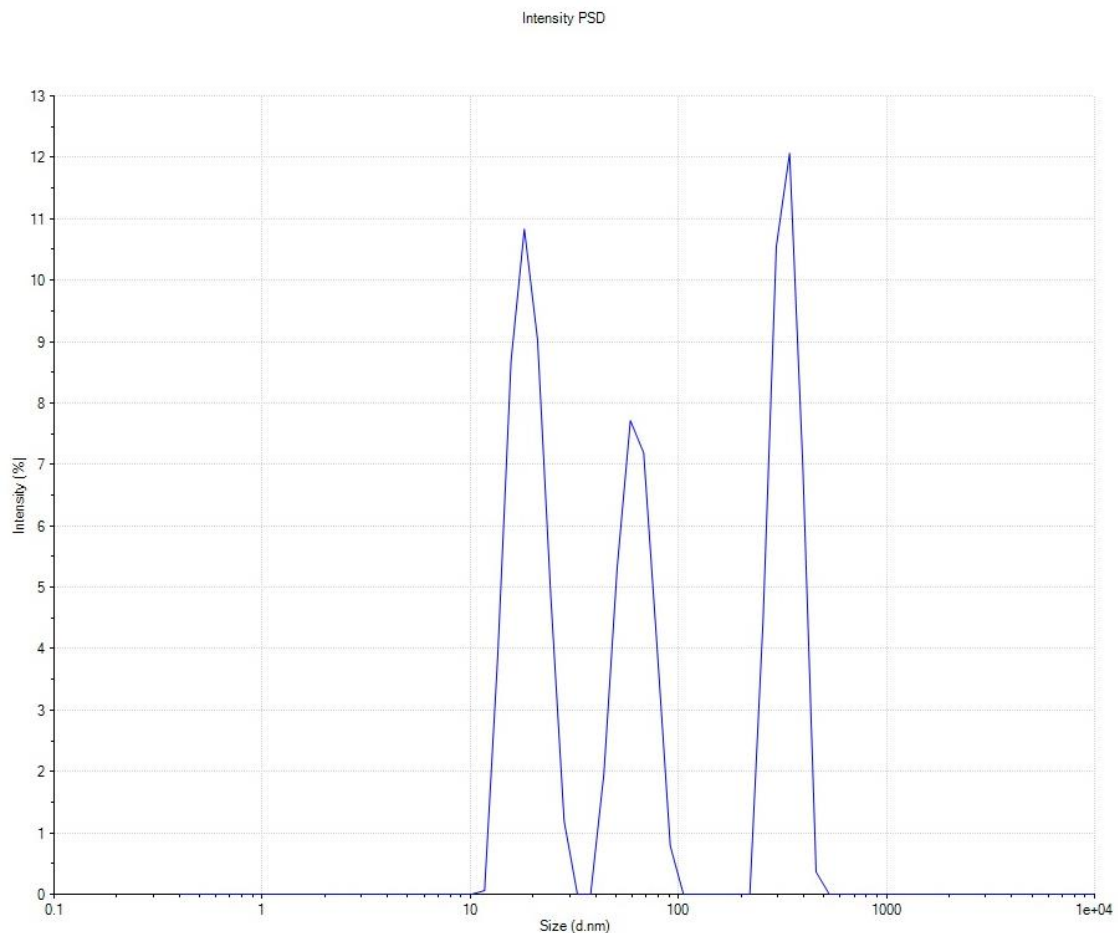
Graph 5: Size of particles after the stabilization with solution of Gum Arabic in lavender essential oil (Intensity).
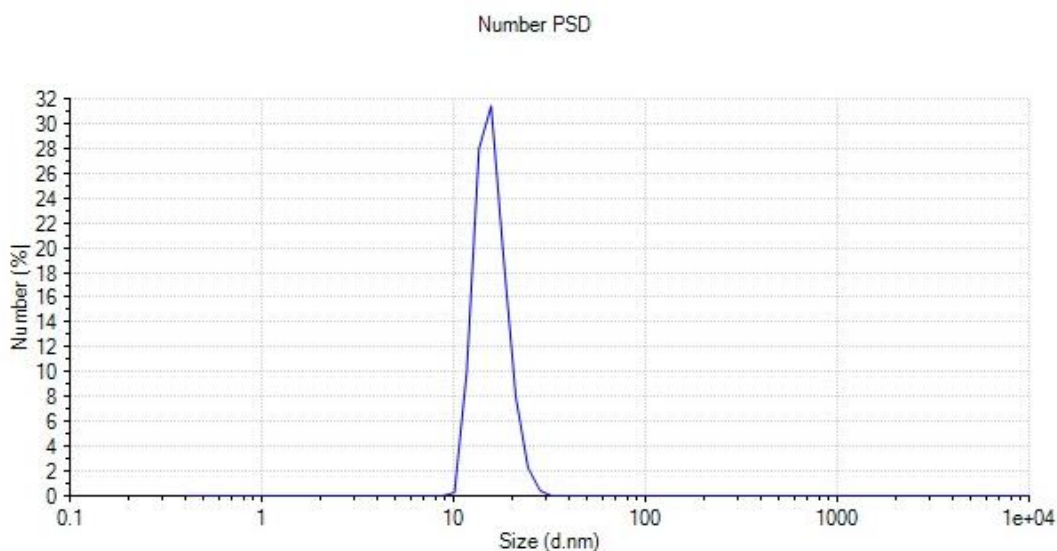
Graph 6: Size of particles after the stabilization with solution of Gum Arabic in lavender essential oil (Number).

As can be seen in the Graph 5 only about a 11% of the particles have a size less than 30nm, while in the Graph 6 almost the 32% of the particles have this size. This is because the phenomenon explained earlier, so is more accurate look at the graphs with "number" in their y axis.

In conclusion, the results obtained whit lavender essential oils are interesting because the size of the nanoparticles is adequate for the applications described before and allows the obtainment of particles with size nano. Furthermore, lavender essential oil has health benefits so that makes prepared nanoparticles more interesting for medical applications. Both procedures resulted in obtainment of nanoparticles so is not possible to choose only one procedure. Although the introduction of lavender essential oil affects significantly the results of the synthesis of the magnetic nanoparticles.

Because of the good results it wasn't necessary to apply ultrasound to disperse the agglomerations. In case of the addition of lavender essential oil the results proved the proper size of the particles, also any polydispersity was observed and it has an impact on the size and distribution of obtained nanoparticles. This increases potential fields of application of such nanoparticles due to the interesting properties of such essential oils from a medical and pharmaceutical point of view.

9 Summary

Magnetic nanoparticles are of great interest for researchers for its wide range of applications. There are different methods of synthesis and the results vary depending on the method used. In this case magnetic nanoparticles were obtained by the method of co-precipitation using Massart synthesis, also it was added lavender essential oils to check if it affects to the final results. The size of the particles was determinated by Dynamic light scattering (DLS) showing that the method and the materials used were suitable for the obtainment of magnetic nanoparticles. It was concluded that the introduction of the lavender essential oil modifies significantly the results but by both procedures was possible to obtain magnetic nanoparticles with the proper size. No additional procedures like ultrasounds to dissolve agglomerations were needed son this indicates that the use of essential oils improves the obtainment of magnetic nanoparticles.

Multiple applications are under investigation, but the most important are in the field of medicine. With these magnetic nanoparticles it is possible to detect and treat several diseases like cancer. The fact that magnetic nanoparticles can be drug carriers make them attractive for their use in medicine. In contrast, the possible toxicity is under study. The levels of toxicity are highly controlled by the regulatory legislature. The coalescence of bioengineering, biomedical and toxicology disciplines will foster development of relevant strategies to engineer advanced magnetic nanoparticle formulations and nanodevices with biocompatible interfaces.

10 References

[1] An-Hui Lu, E. L. Salabas, and Ferdi Schüth, Magnetic Nanoparticles: Synthesis, Protection, Functionalization, and Application, *Angew. Chem. Int. Ed.* **2007**, 46, 1222 – 1244

[2] En.wikipedia.org. (2018). Magnetic nanoparticles. [online] Available at: https://en.wikipedia.org/wiki/Magnetic_nanoparticles#Co-precipitation

[3] Cameo.mfa.org. (2018). Gum arabic - CAMEO. [online] Available at: http://cameo.mfa.org/wiki/Gum_arabic

[4] Organic Facts. (2018). List of Essential Oils | Organic Facts. [online] Available at: https://www.organicfacts.net/health-benefits/essential-oils

[5] E. L. Salabas, A. Rumplecker, F. Kleitz, F. Radu, F. SchVth, Nano Lett. **2006**, 6, 2977.

[6] Y. Wang, C.-M. Yang, W. Schmidt, B. Spliethoff, E. Bill, F. SchVth, Adv. Mater. **2005**, 17, 53.

[7] Y. Li, M. Afzaal, P. O=Brien, J. Mater. Chem. **2006**, 16, 2175.

[8] C. Stinner, R. Prins, T. Weber, J. Catal. **2001**, 202, 187.

[9] P. A. Dresco, V. S. Zaitsev, R. J. Gambino, B. Chu, Langmuir **1999**, 15, 1945.

[10] B. L. Frankamp, N. O. Fischer, R. Hong, S. Srivastava, V. M. Rotello Chem. Mater. **2006**, 18, 956.

[11] Y. Kobayashi, M. Horie, M. Konno, B. Rodriguez-GonzXlez, L. M. Liz-Marzan, J. Phys. Chem. B **2003**, 107, 7420.

[12] S. Sun, C. B. Murray, D. Weller, L. Folks, A. Moser, Science 2000, 287, 1989.

[13] F. Caruso, M. Spasova, A. Susha, M. Giersig, R. A. Caruso, Chem. Mater. **2001**, 13, 109.

[14] K. H. Ang, I. Alexandrou, N. D. Mathur, G. A. J. Amaratunga, S. Haq, Nanotechnology **2004**, 15, 520.

[15] M. A. Correa-Duarte, M. Giersig, N. A. Kotov, L. M. Liz-Marzán, Langmuir **1998**, 14, 6430.

[16] Nature of Europe. (2018). Essential Oils - Nature of Europe. [online] Available at: http://natureofeurope.com/essential-oils/

[17] Organic Facts. (2018). 13 Surprising Benefits of Lavender Essential Oil | Organic Facts. [online] Available at: https://www.organicfacts.net/health-benefits/essential-oils/health-benefits-of-lavender-essential-oil.html

[18]   Shubayev, V., Pisanic, T. and Jin, S. Magnetic nanoparticles for theragnostics. Advanced Drug Delivery Reviews, 61(6), **2009**, pp.467-477.